C1: Recent Developments of the KOSMA-τ PDR Code

M. Röllig
V. Ossenkopf, R. Szczerba, Z. Makai, C. Glück,
Y. Okada, S. Andree

Universität zu Köln, Germany

Introduction to KOSMA-τ

- Sub-project C1:

  „Modeling of irradiated molecular clouds“

- PI: Volker Ossenkopf

Introduction to KOSMA-τ

- PDR stands for
  - Photo-Dissociation Region
  - Photon Dominated Region

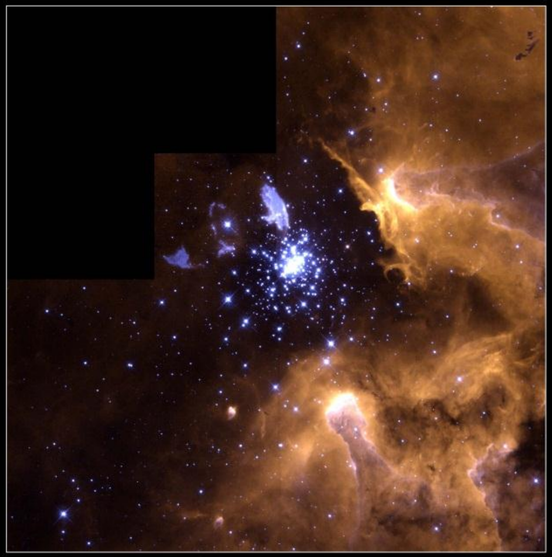

NGC 3603
Hubble Space Telescope • WFPC2

PRC99-20 • STScI OPO
Wolfgang Brandner (JPL/IPAC), Eva K. Grebel (University of Washington),
You-Hua Chu (University of Illinois, Urbana-Champaign) and NASA

- A region where far-ultraviolett (FUV) photons from young, massive stars dominate the physics and chemistry of the interstellar medium

Introduction to KOSMA-τ

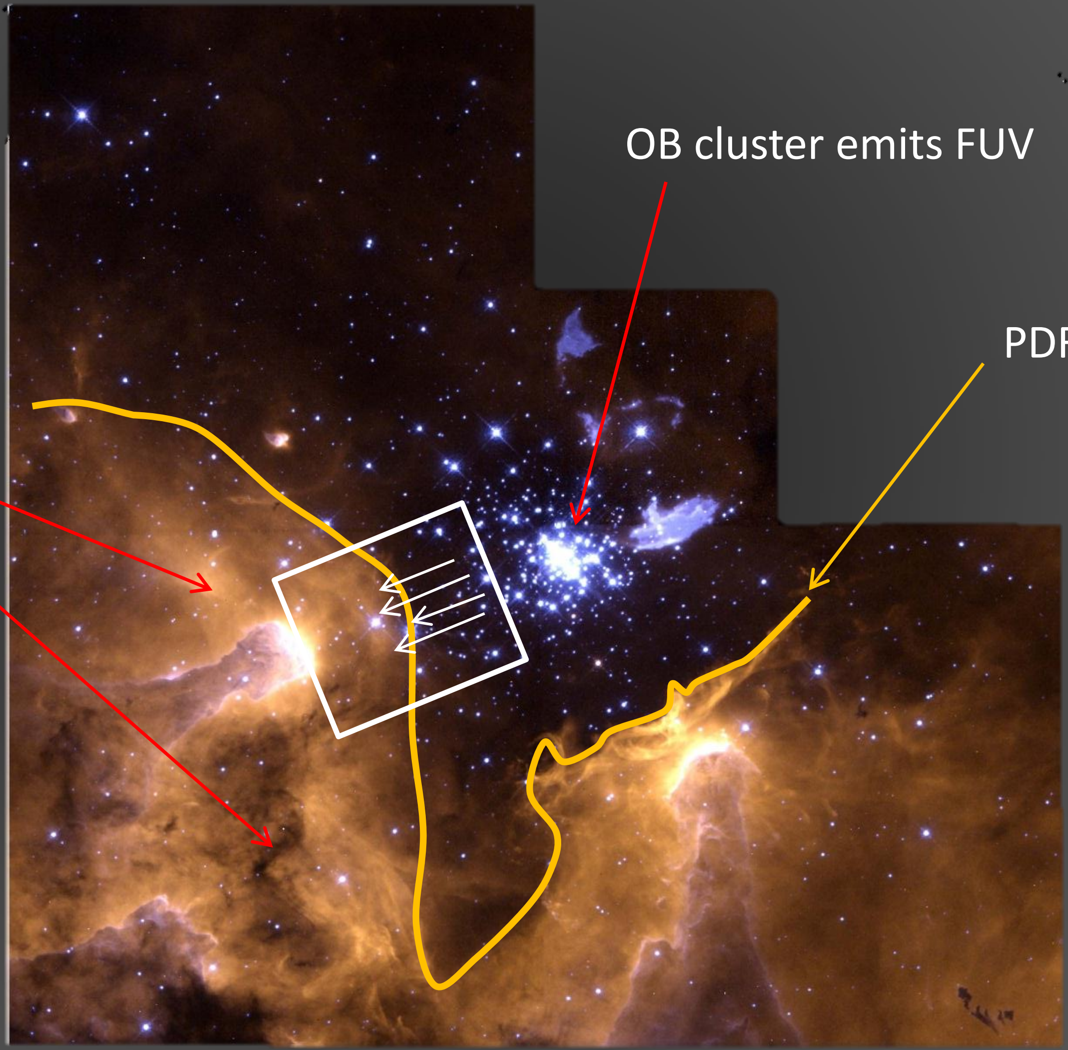

OB cluster emits FUV

molecular cloud
contains gas & dust

PDR interface

Introduction to KOSMA-τ

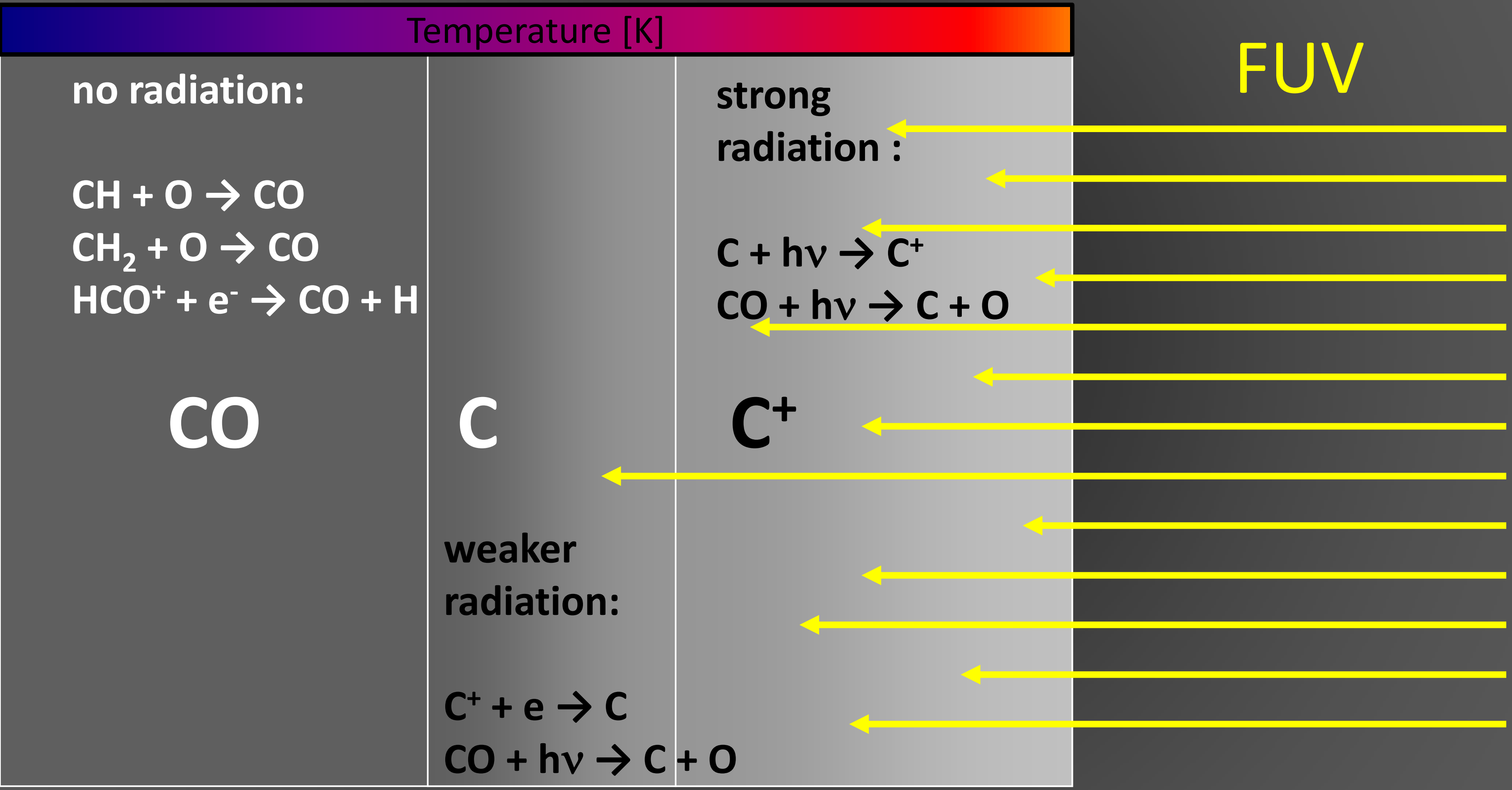

no radiation:

$CH + O \rightarrow CO$
$CH_2 + O \rightarrow CO$
$HCO^+ + e^- \rightarrow CO + H$

CO

C

weaker radiation:

$C^+ + e \rightarrow C$
$CO + h\nu \rightarrow C + O$

strong radiation :

$C + h\nu \rightarrow C^+$
$CO + h\nu \rightarrow C + O$

C^+

Interstellar cloud surface (cross section)

Modeling: KOSMA-τ PDR Code

- spherical geometry

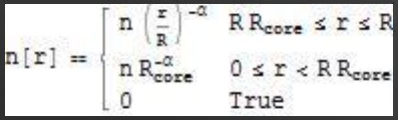

$$n[r] == \begin{cases} n\left(\frac{r}{R}\right)^{-\alpha} & R\,R_{core} \le r \le R \\ n\,R_{core}^{-\alpha} & 0 \le r < R\,R_{core} \\ 0 & True \end{cases}$$

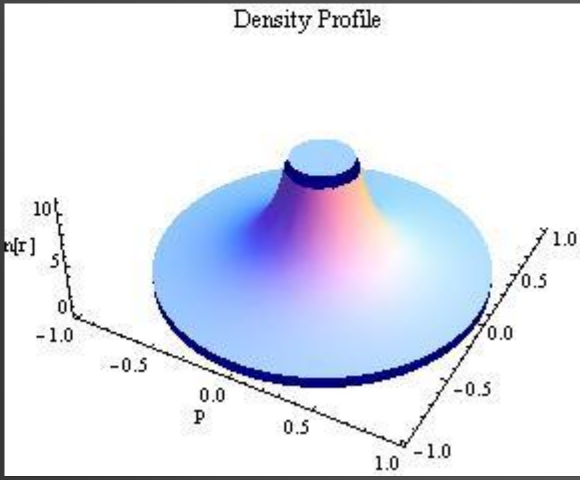

- isotropic illumination
- modular chemistry incl. isotopologues
- coupled with radiative transfer code (MCDRT, ONION, SimLine, etc.)
- self-consistently solves chemistry & energy balance

Modeling: KOSMA-τ PDR Code

Output:

- density profile of all contained species
- temperature profile (gas, dust)
- excitation conditions (T_{ex}, etc.)
- clump-averaged quantities
  - column densities
  - AV
  - optical depths
  - intensities

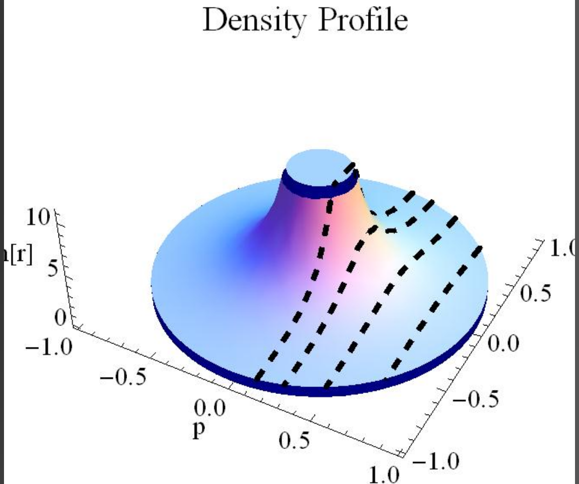

Modeling: KOSMA-τ PDR Code

- But: Molecular clouds are not spherical (nor plane-parallel)
- Idea: compose non-spherical clouds from spherical clumps

Clumpy Clouds via Superposition of Individual Clouds

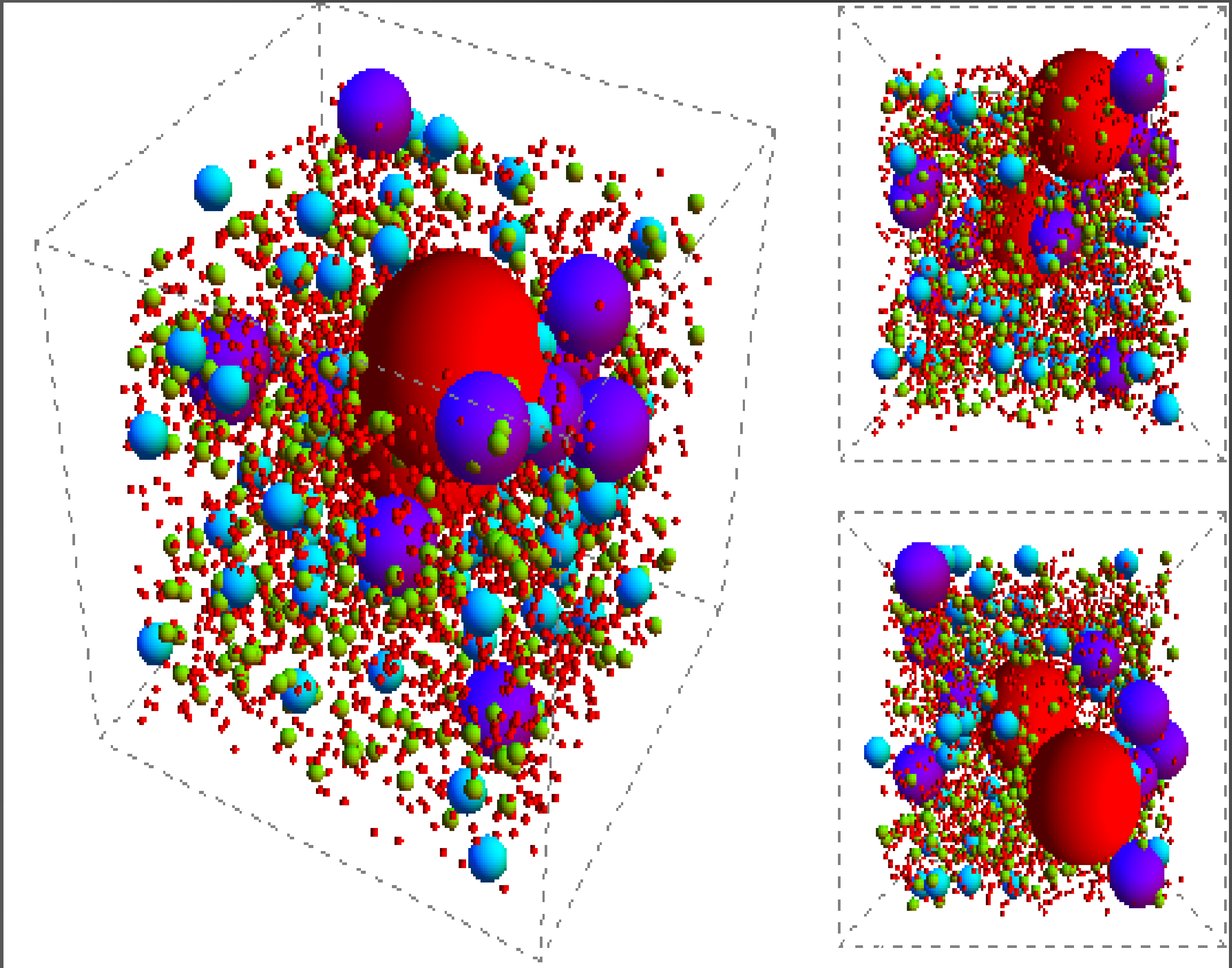

$dN/dM \sim M^{-1.8}$

$M/M_\odot$	N
100	2
10	13
1	80
0.1	502
0.01	3170

$M_{tot}=673\ M_\odot$

Clumpy Media

- random realisation of an ensemble with $M_{tot}=10^4 M_\odot$ (subdivided into 4 condensations)

Pillars in Rosette (HOBYS team: Motte et al. 2010)

random distribution

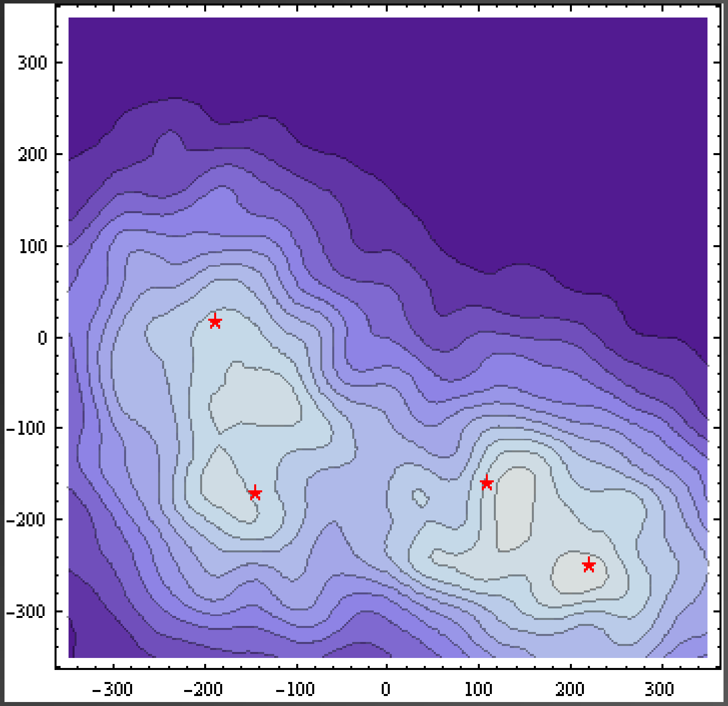

observed with a 45'' beam

Update of chemical modeling

Introduction

“garbage” in – garbage out

- missing experimental data
- inter/extrapolation

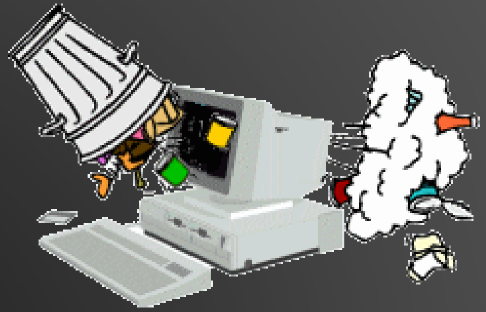

“OK, if you’re so smart, *you* manage the portfolio!”

UMIST/UDfA - Isotopomers

- Insert a single ^{13}C and/or ^{18}O into the UDfA reeactions
- Automatic introduction of isotopes into chemical compounds is not easy. Simple permutation may lead to undesired reactions

blind permutation

CH3	CN$^-$	· · ⟩	CH3CN	e$^-$
CH3	13CN$^-$	· · ⟩	CH313CN	e$^-$
CH3	13CN$^-$	· · ⟩	13CH3CN	e$^-$
13CH3	CN$^-$	· · ⟩	CH313CN	e$^-$
13CH3	CN$^-$	· · ⟩	13CH3CN	e$^-$

‚cleverer' permutation

CH3	CN$^-$	· · ⟩	CH3CN	e$^-$
CH3	13CN$^-$	· · ⟩	CH313CN	e$^-$
13CH3	CN$^-$	· · ⟩	13CH3CN	e$^-$

functional group binding needs to be kept

UMIST/UDfA - Isotopomers

Complexity is large. Blind permutation of UDfA06 leads to ~50000 reactions! Automatic house-keeping necessary.

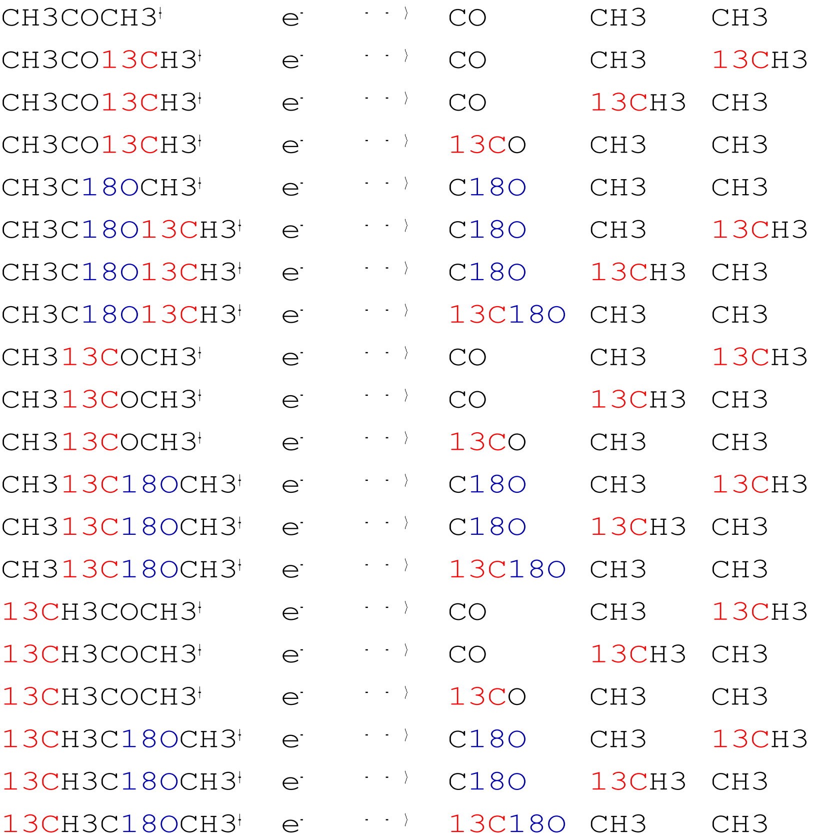

CH3COCH3+	e-	→	CO	CH3	CH3
CH3CO13CH3+	e-	→	CO	CH3	13CH3
CH3CO13CH3+	e-	→	CO	13CH3	CH3
CH3CO13CH3+	e-	→	13CO	CH3	CH3
CH3C18OCH3+	e-	→	C18O	CH3	CH3
CH3C18O13CH3+	e-	→	C18O	CH3	13CH3
CH3C18O13CH3+	e-	→	C18O	13CH3	CH3
CH3C18O13CH3+	e-	→	13C18O	CH3	CH3
CH313COCH3+	e-	→	CO	CH3	13CH3
CH313COCH3+	e-	→	CO	13CH3	CH3
CH313COCH3+	e-	→	13CO	CH3	CH3
CH313C18OCH3+	e-	→	C18O	CH3	13CH3
CH313C18OCH3+	e-	→	C18O	13CH3	CH3
CH313C18OCH3+	e-	→	13C18O	CH3	CH3
13CH3COCH3+	e-	→	CO	CH3	13CH3
13CH3COCH3+	e-	→	CO	13CH3	CH3
13CH3COCH3+	e-	→	13CO	CH3	CH3
13CH3C18OCH3+	e-	→	C18O	CH3	13CH3
13CH3C18OCH3+	e-	→	C18O	13CH3	CH3
13CH3C18OCH3+	e-	→	13C18O	CH3	CH3

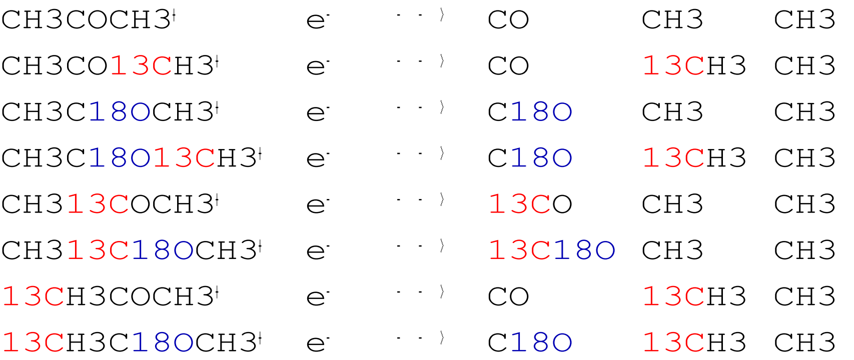

CH3COCH3+	e-	→	CO	CH3	CH3
CH3CO13CH3+	e-	→	CO	13CH3	CH3
CH3C18OCH3+	e-	→	C18O	CH3	CH3
CH3C18O13CH3+	e-	→	C18O	13CH3	CH3
CH313COCH3+	e-	→	13CO	CH3	CH3
CH313C18OCH3+	e-	→	13C18O	CH3	CH3
13CH3COCH3+	e-	→	CO	13CH3	CH3
13CH3C18OCH3+	e-	→	C18O	13CH3	CH3

UMIST/UDfA - Isotopomers

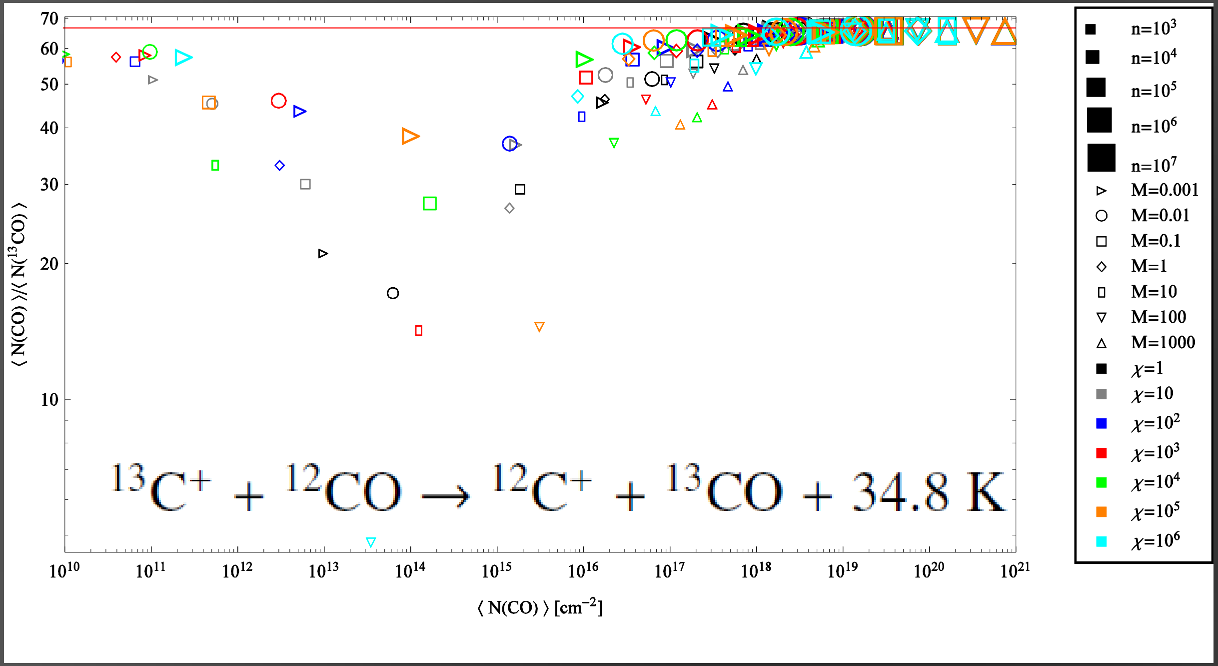

$$^{13}C^+ + {}^{12}CO \rightarrow {}^{12}C^+ + {}^{13}CO + 34.8\ K$$

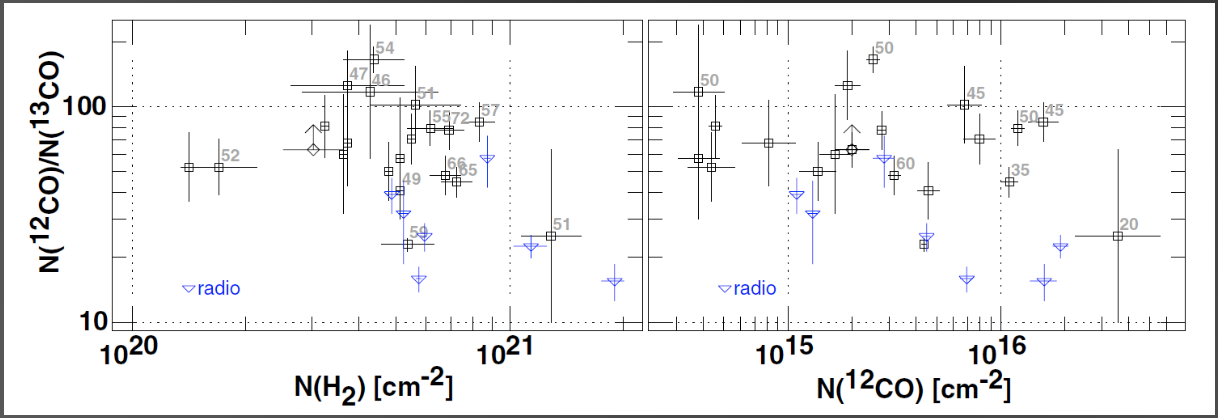

Chemistry : FR<ER

Photodissoc.: FR>ER

Models indicate no fractionation of CO c towards FR>ER

Isotope exchange chemistry always dominates over isotope selective photodissociation

Data from diffuse clouds show both cases

Liszt 2007

Refit to problematic reaction rates

Refit to problematic reaction rates

- chemical reaction rate coefficients are usually parametrized using few parameters (which are tabulated in chemical databases), e.g. α, β, γ

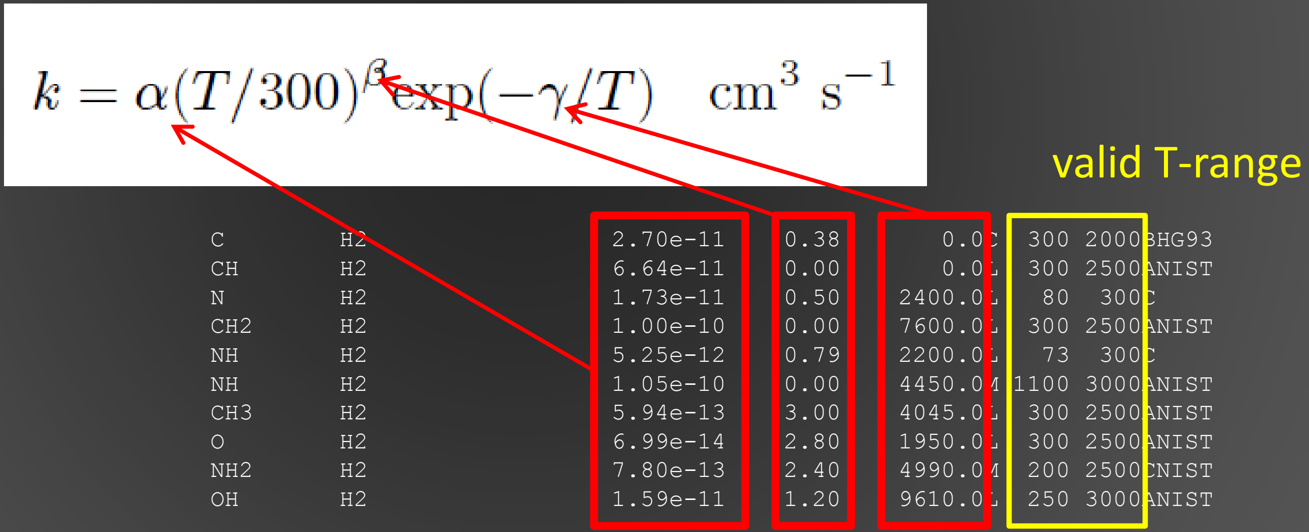

$$k = \alpha (T/300)^{\beta} \exp(-\gamma/T) \quad \mathrm{cm}^3\ \mathrm{s}^{-1}$$

```
  1 H        CH          C        H2        2.70e-11  0.38     0.0C  300  2000BHG93
  2 H        CH2         CH       H2        6.64e-11  0.00     0.0L  300  2500ANIST
  3 H        NH          N        H2        1.73e-11  0.50  2400.0L   80   300C
  4 H        CH3         CH2      H2        1.00e-10  0.00  7600.0L  300  2500ANIST
  5 H        NH2         NH       H2        5.25e-12  0.79  2200.0L   73   300C
  6 H        NH2         NH       H2        1.05e-10  0.00  4450.0M 1100  3000ANIST
  7 H        CH4         CH3      H2        5.94e-13  3.00  4045.0L  300  2500ANIST
  8 H        OH          O        H2        6.99e-14  2.80  1950.0L  300  2500ANIST
  9 H        NH3         NH2      H2        7.80e-13  2.40  4990.0M  200  2500CNIST
 10 H        H2O         OH       H2        1.59e-11  1.20  9610.0L  250  3000ANIST
```

- α, β, γ from best fit to experimental data within the experiments temperature range!

Negative γ

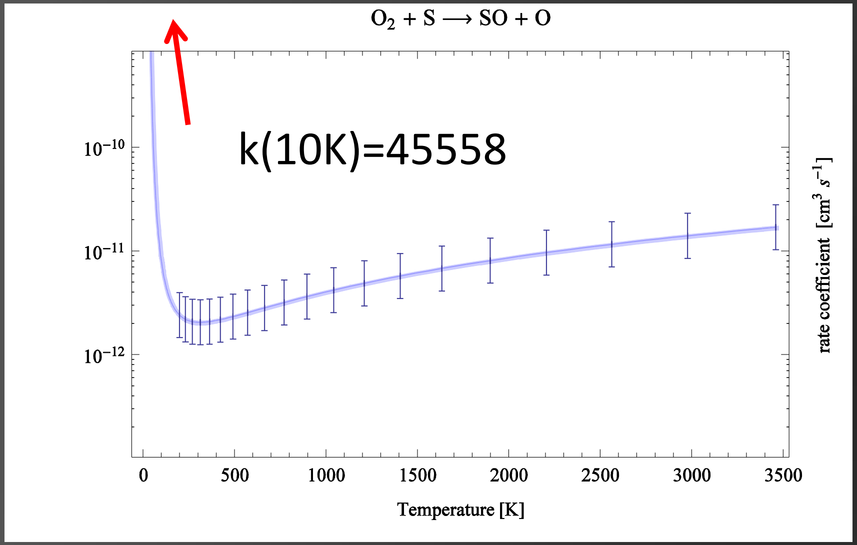

$O_2 + S \longrightarrow SO + O$

k(10K)=45558

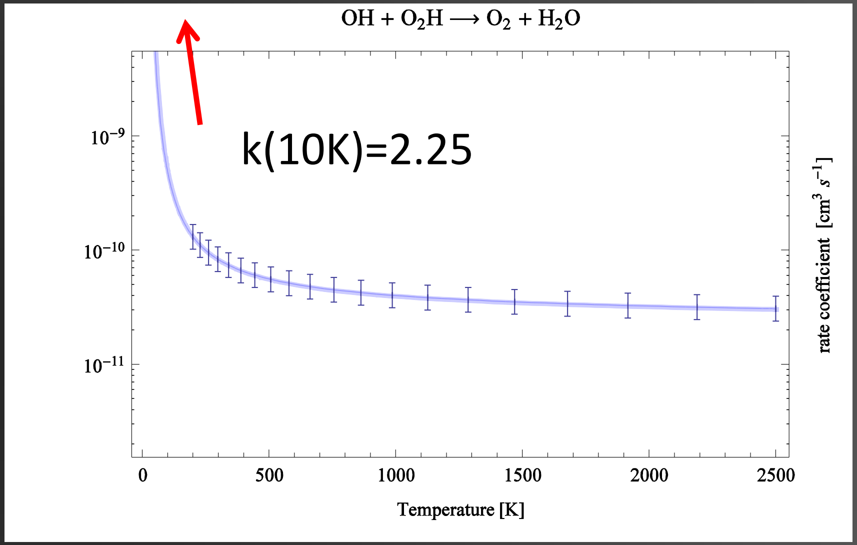

$OH + O_2H \longrightarrow O_2 + H_2O$

k(10K)=2.25

- Outside their temperature regime, the rate coefficient may become unrealistically large
- one suggested remedy: k(10K)→0

Negative γ

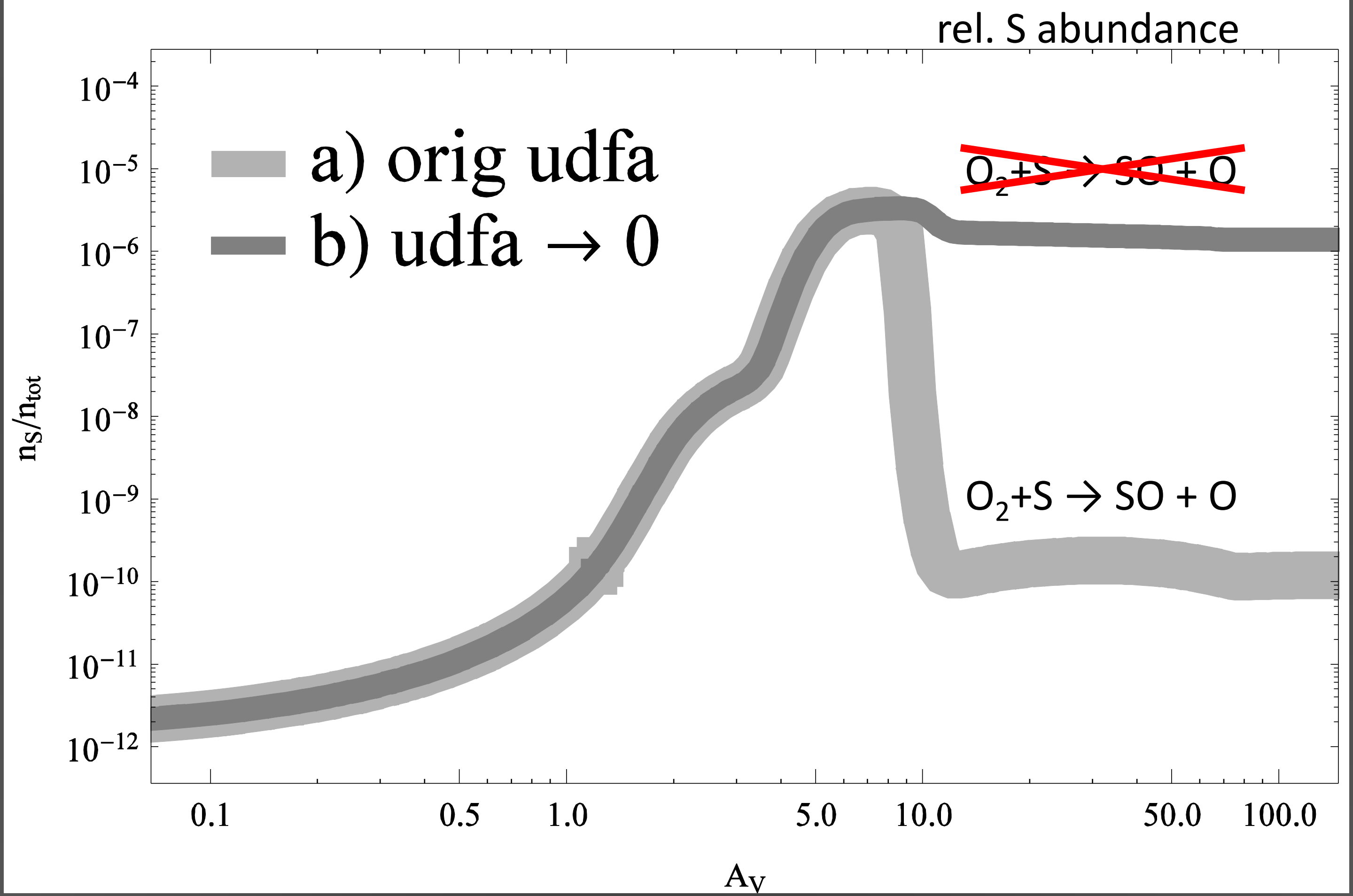

KOSMA-τ model result

Negative γ

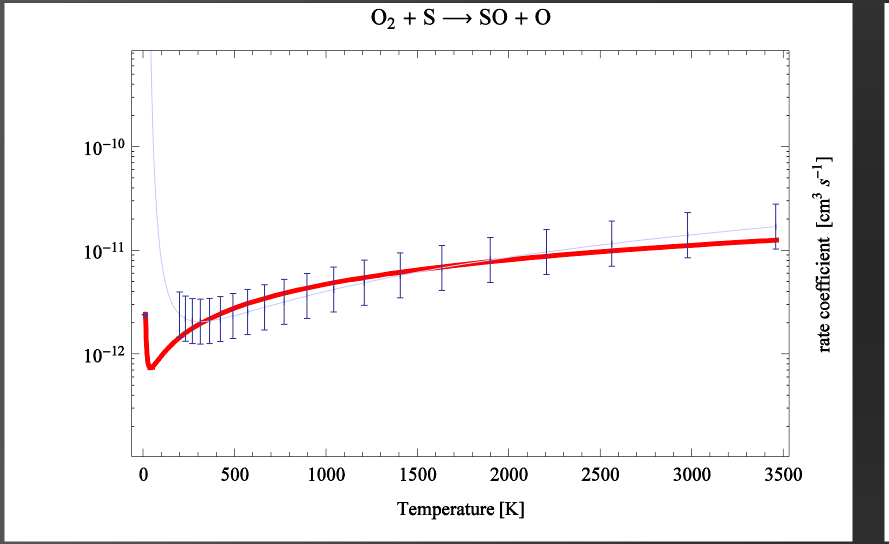

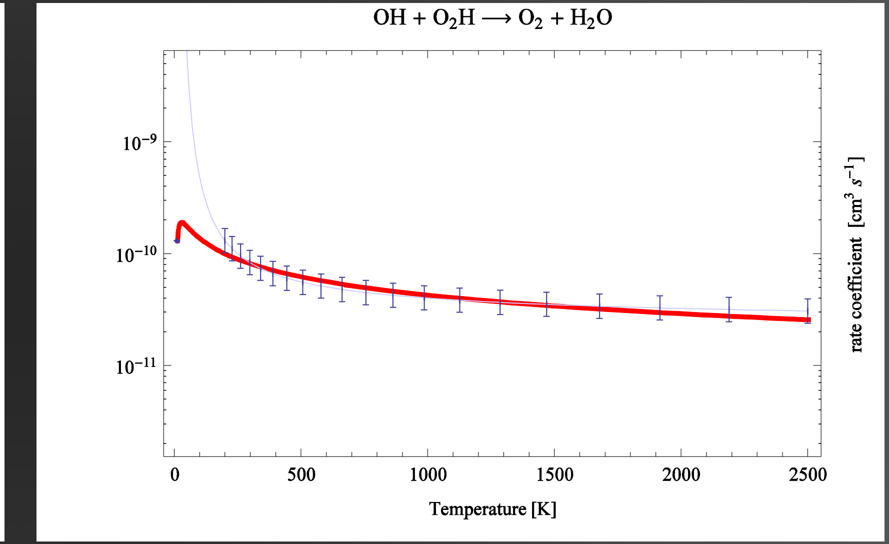

- forcing the fit with an artificial, low T „data point“
- stay inside the original error bars as much as possible
- choice of k(10K) is arbitrary and a possibly large error source!

Negative γ

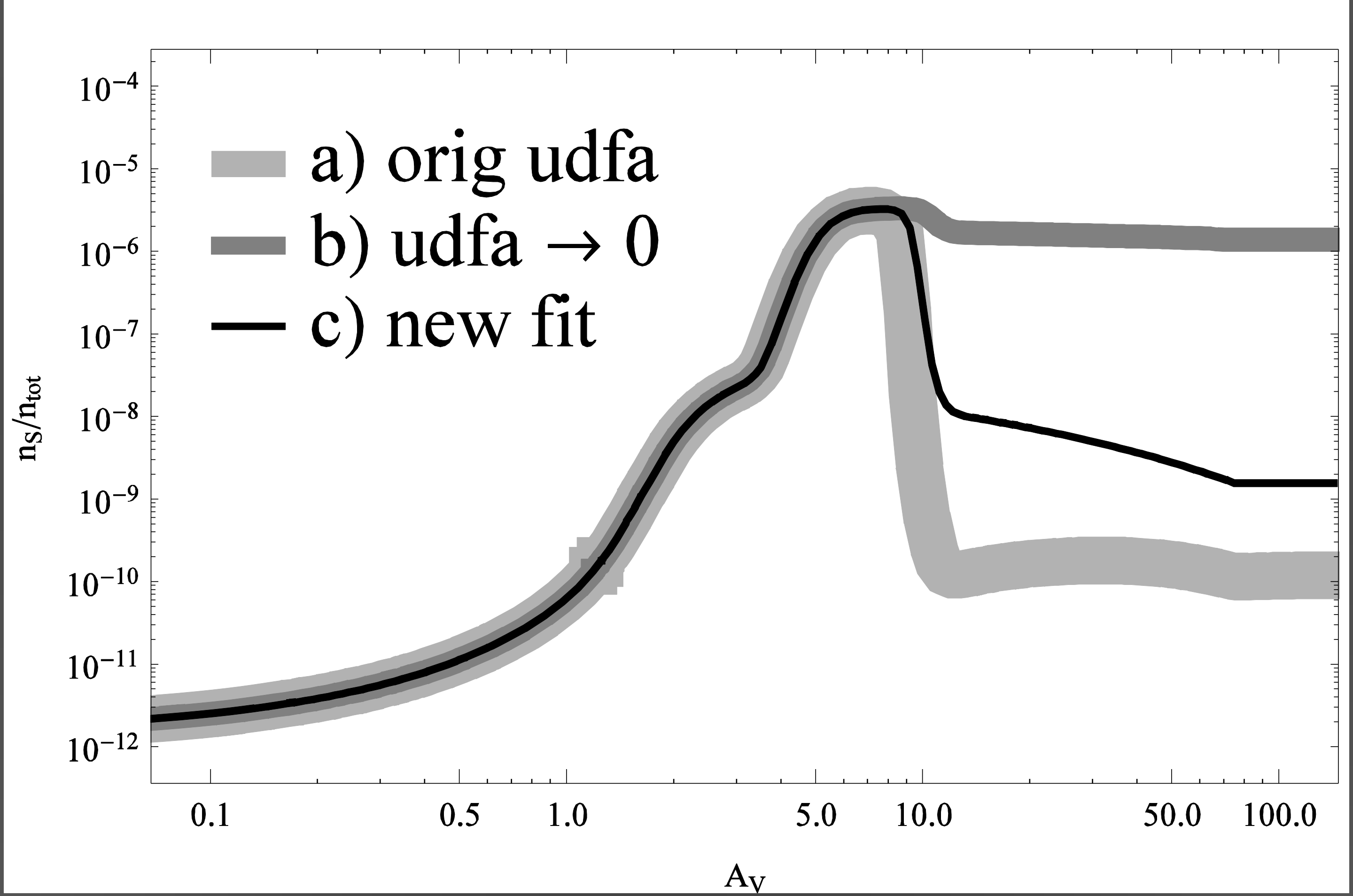

Self consistent dust modelling

Self consistent dust modelling

- Interstellar dust covers only 1% of the total mass of a molecular cloud.
- However, dust controls many astrophysical key processes:
  - FUV continuum radiative transfer
  - Photo-electric heating is major heating term
  - Grain surface chemistry → e.g. H_2 formation
- Coupling: KOSMA-τ ⇔ MCDRT-code

Multi-**C**omponent-**D**ust-**R**adiative-**T**ransfer **C**ode
(R. Szczerba)

Self consistent dust modelling

The dust properties in the ISM remain one of the major unknowns in modern astronomy.

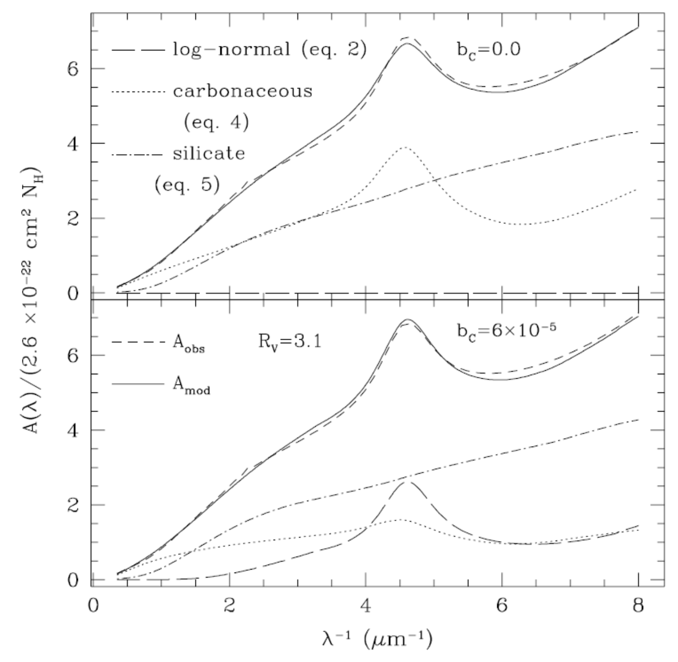

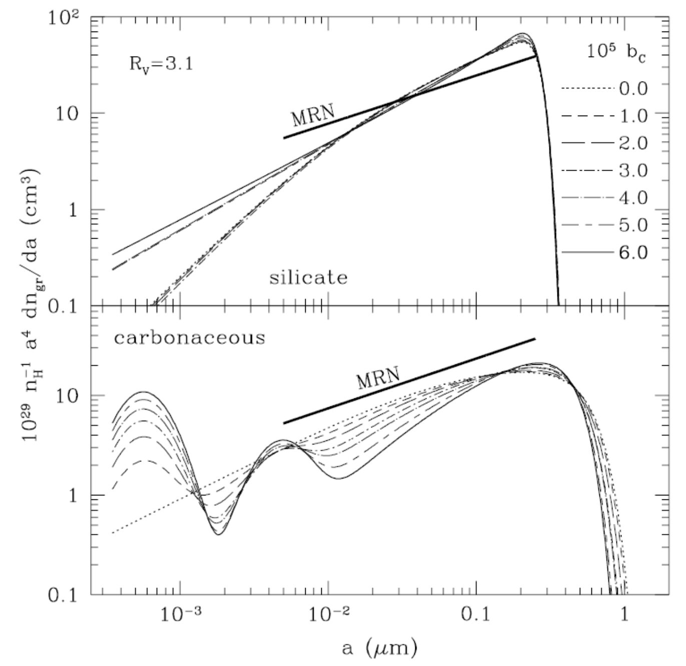

Weingartner & Draine 2001, ApJ 548

Fit to extinction curve

different material and size distributions

Self consistent dust modelling

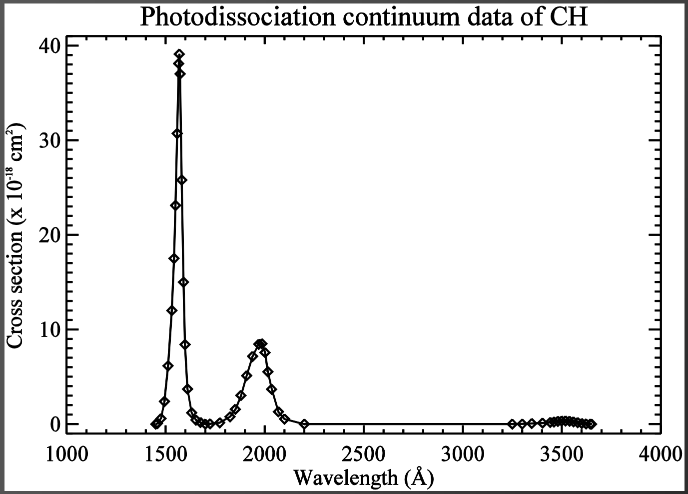

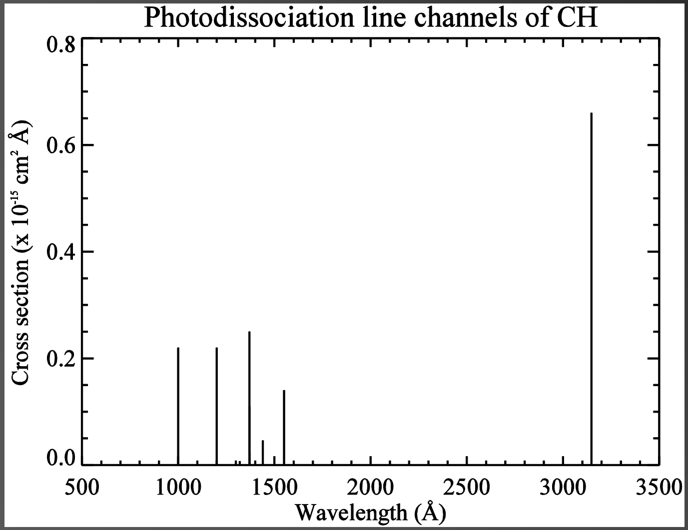

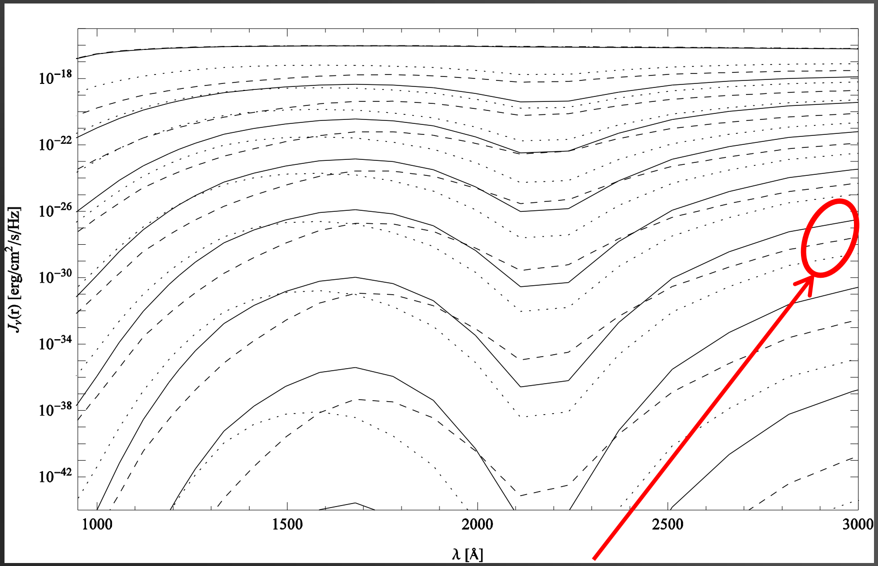

different dust models

$$k_{pd}^{cont} = \int \sigma_{ud}(\lambda) x_l I(\lambda) d\lambda \quad s^{-1}$$

Photo-dissociation rate

$$k_{pd}^{line} = \frac{\pi e^2}{mc^2} \lambda_{ud}^2 f_{ud} \eta_u x_l I(\lambda_{ud}) \quad s^{-1}$$

versus

$$k = \alpha \exp(-\gamma A_V) \quad \mathrm{s}^{-1}$$

Self consistent dust modelling

- The dust content is critical for the energy balance
  - Photo-electric heating strongly depends on the dust properties.
  - H_2 formation heating depends on the avaialble surface.

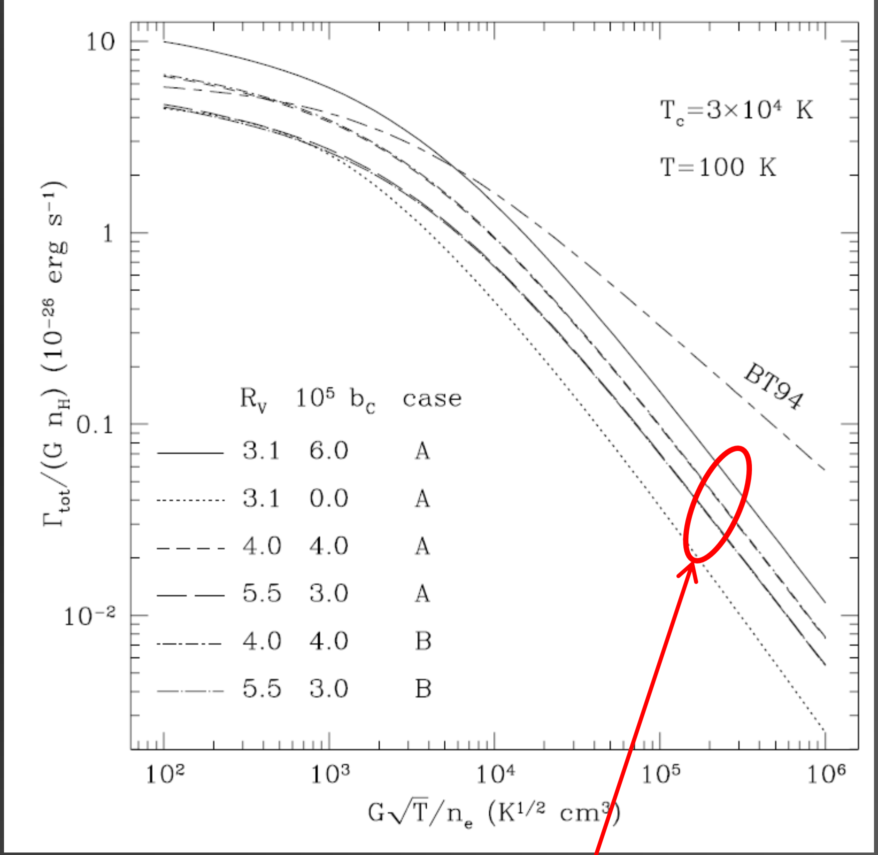

Weingartner & Draine 2001, ApJSS 134

different dust models

Self consistent dust modeling

- Dust continuum emission efficiently cools the gas.
- Prediction of continuum and line emission of a model clump
  → additional observational constraint on the models

- Dust temperature calculated for all dust components and grain sizes

  → prerequisite for grain surface chemistry calculations

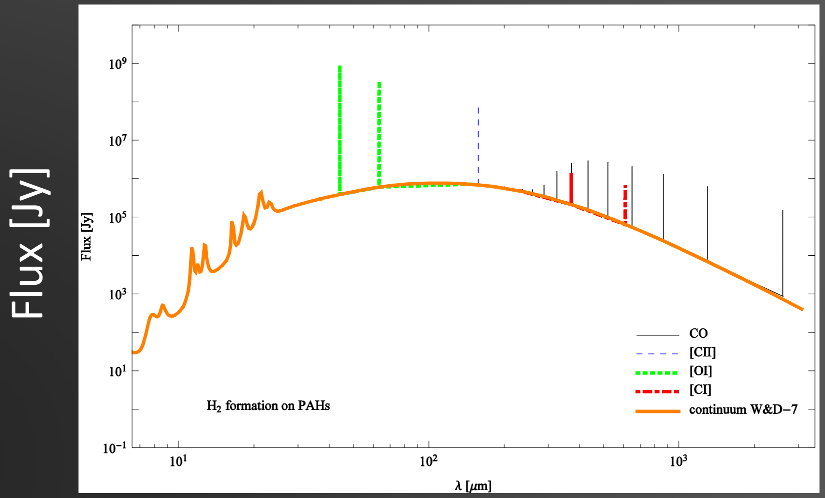

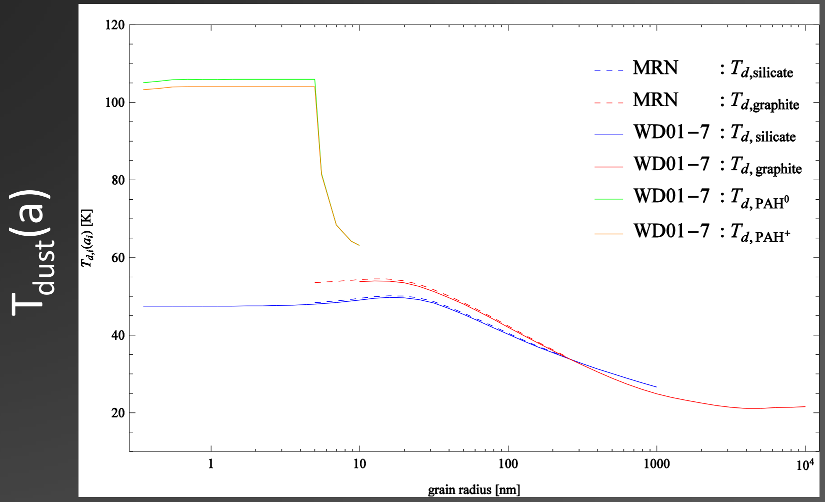

Röllig et al., 2012, submitted

H_2 formation on grain surfaces

H_2 formation on grain surfaces

- H atoms hitting grain surfaces can stick weakly (physisorption) or strongly (chemisorption) bound.
- T_d>100 K desorption overcomes binding and H_2 formation efficiency →0
- Chemisorbed H atoms can effectively form H_2 up to T>500K
- we implemented the formalism presented by Cazaux & Tielens (2002,2004) in the KOSMA-τ chemistry.

H_2 formation efficiency

$$\epsilon_{H_2} = \left(\xcancel{\frac{\mu F}{2\beta_{H_2}}} + 1 + \frac{\beta_{H_P}}{\alpha_{pc}} \right)^{-1}$$

Cazaux & Tielens 2004, ApJ 604

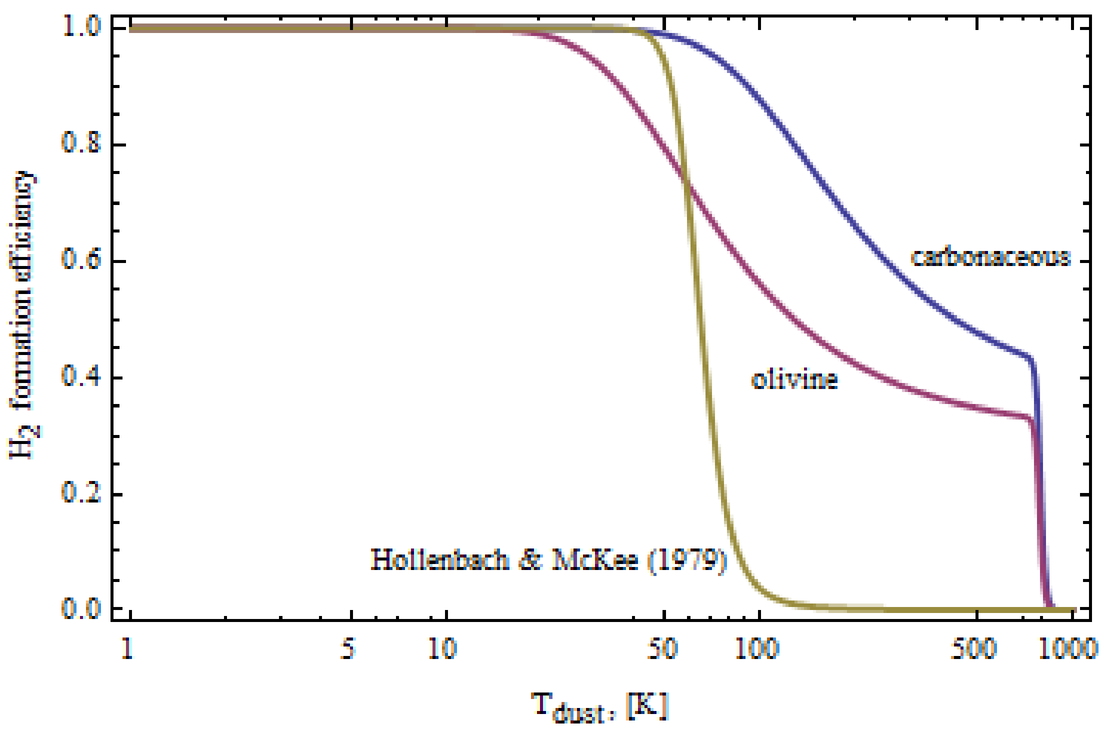

H_2 formation rate

total formation rate depends on total dust surface

$$R_d = \frac{1}{2} n(H) v_H n_d \boxed{\sigma_d} \epsilon_{\mathrm{H}_2} S_H$$

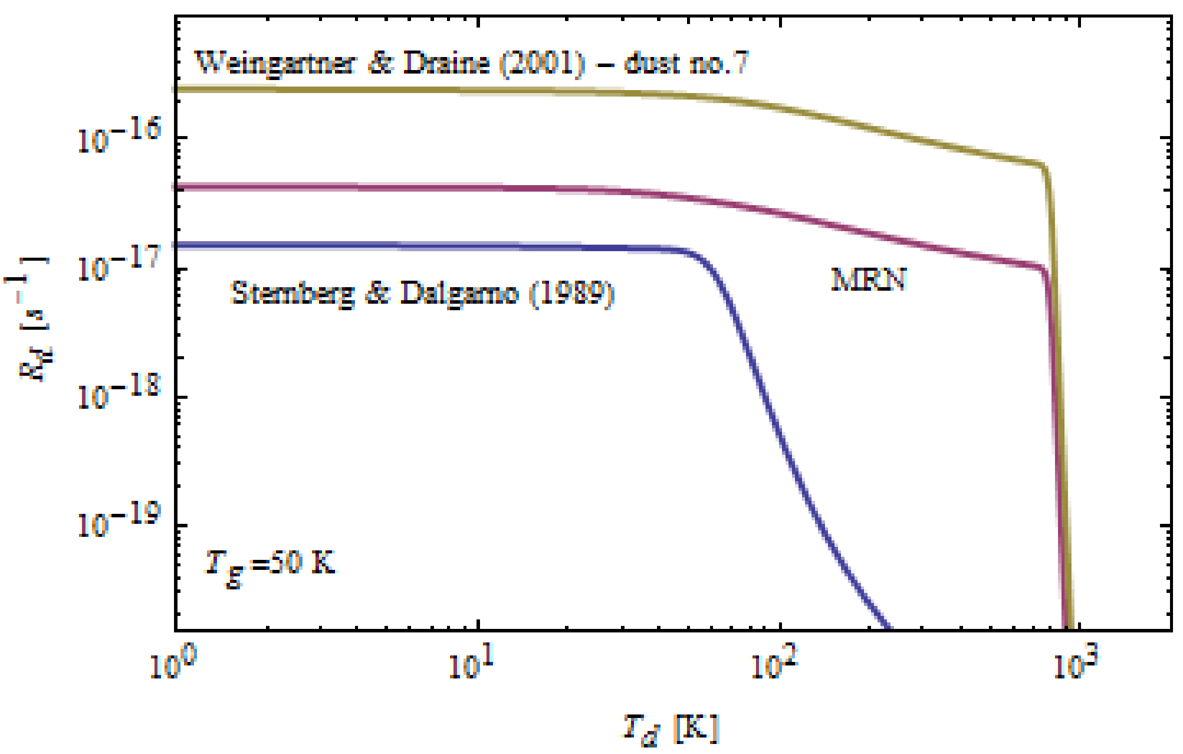

H_2 heating/cooling

- H_2 binding energy 4.5 eV
  → H_2 formation heating
- kinetic H_2 dissociation cooling
  (Lepp & Shull, 1983, ApJ 270, 578)
  $H_2 + H \rightarrow H + H + H - 4.5\text{eV}$
  $H_2 + H_2 \rightarrow H_2 + H + H - 4.5\text{eV}$

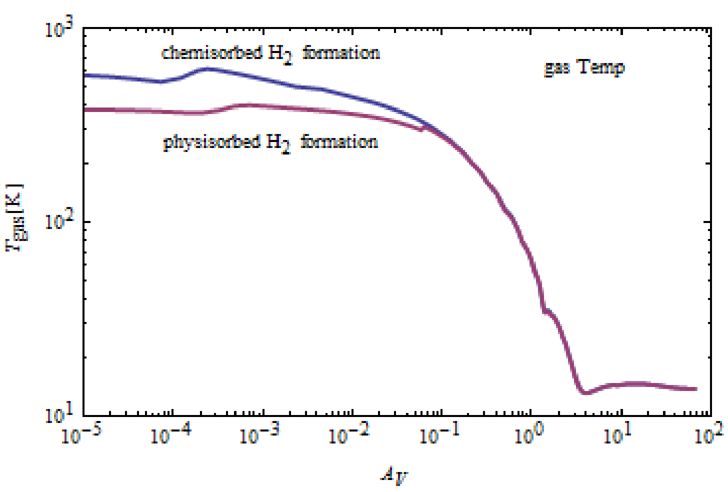

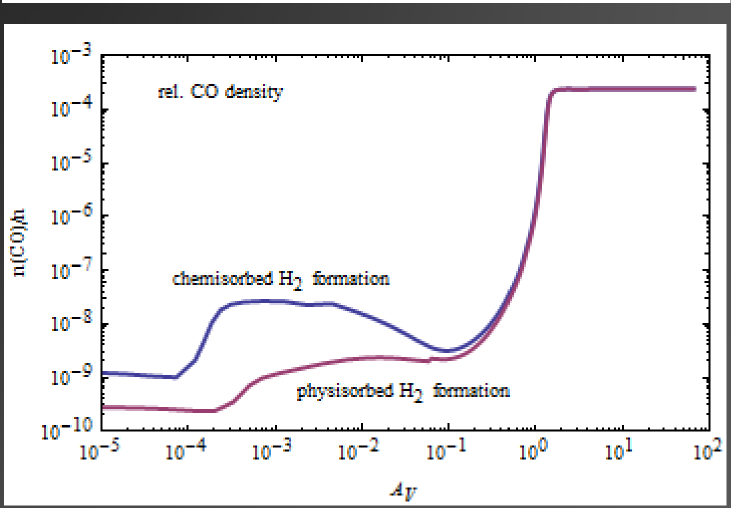

- large effect on H-H_2 transition region chemistry
- chemistry ↔ physics

H_2 Formation on PAHs?

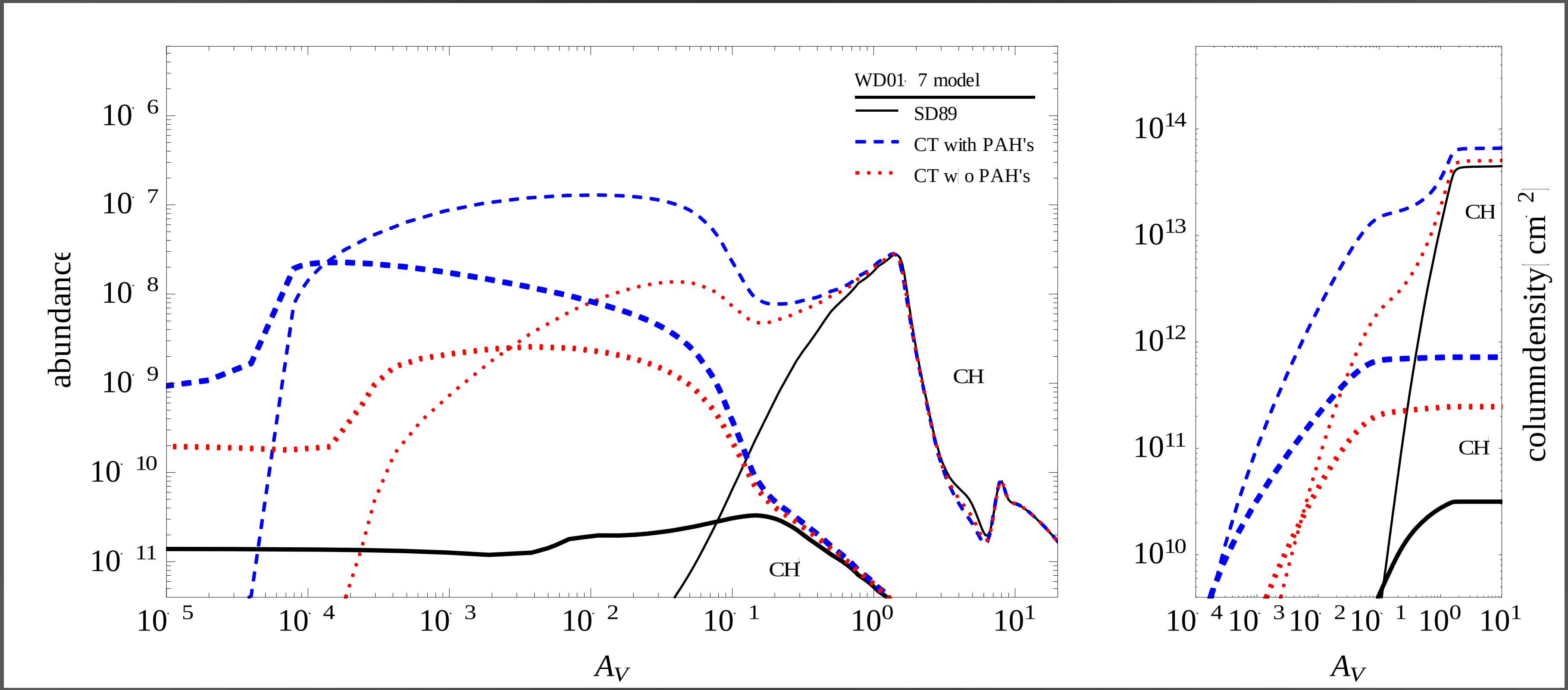

CH column density

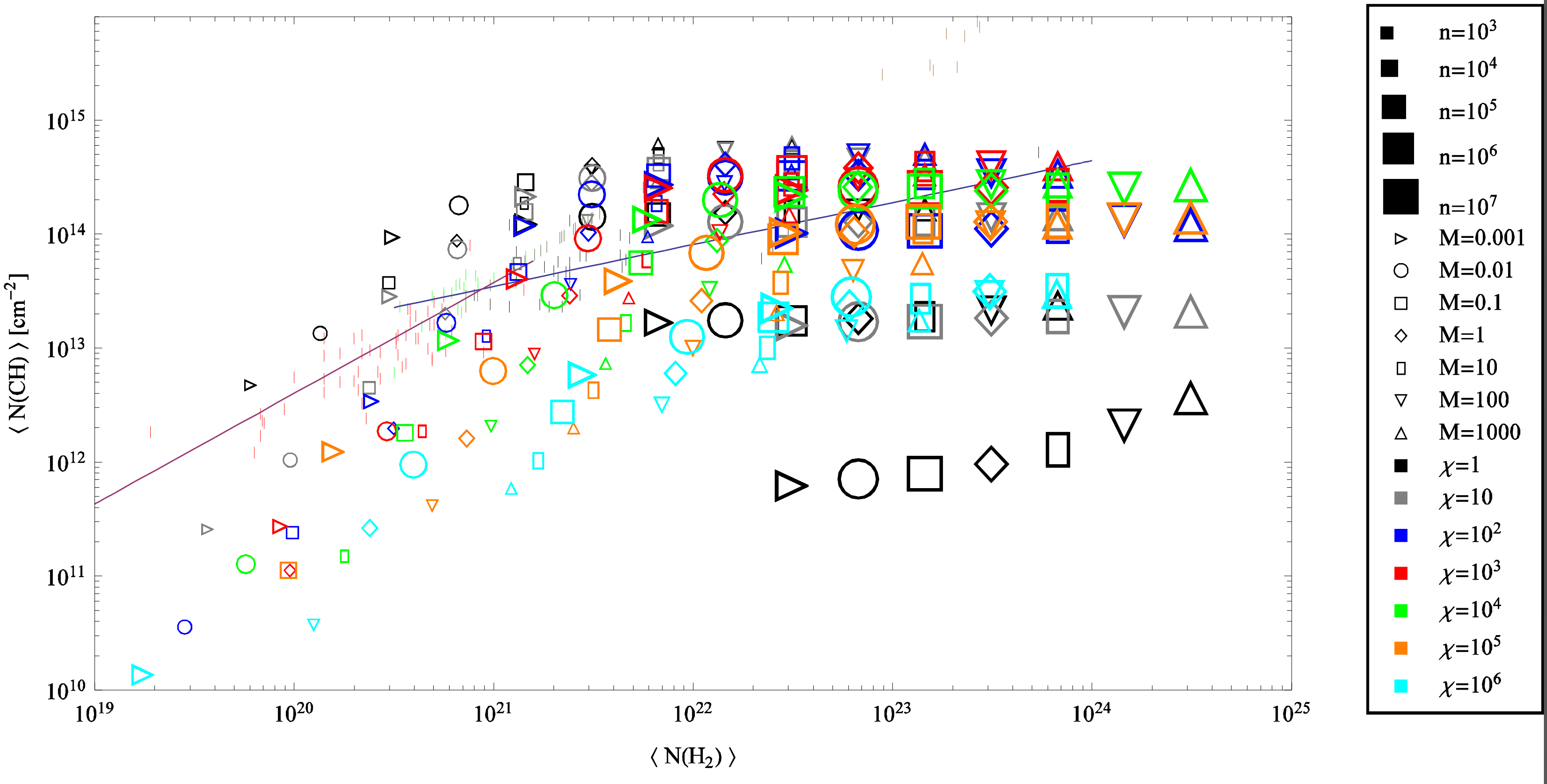

CO Surface Brightness

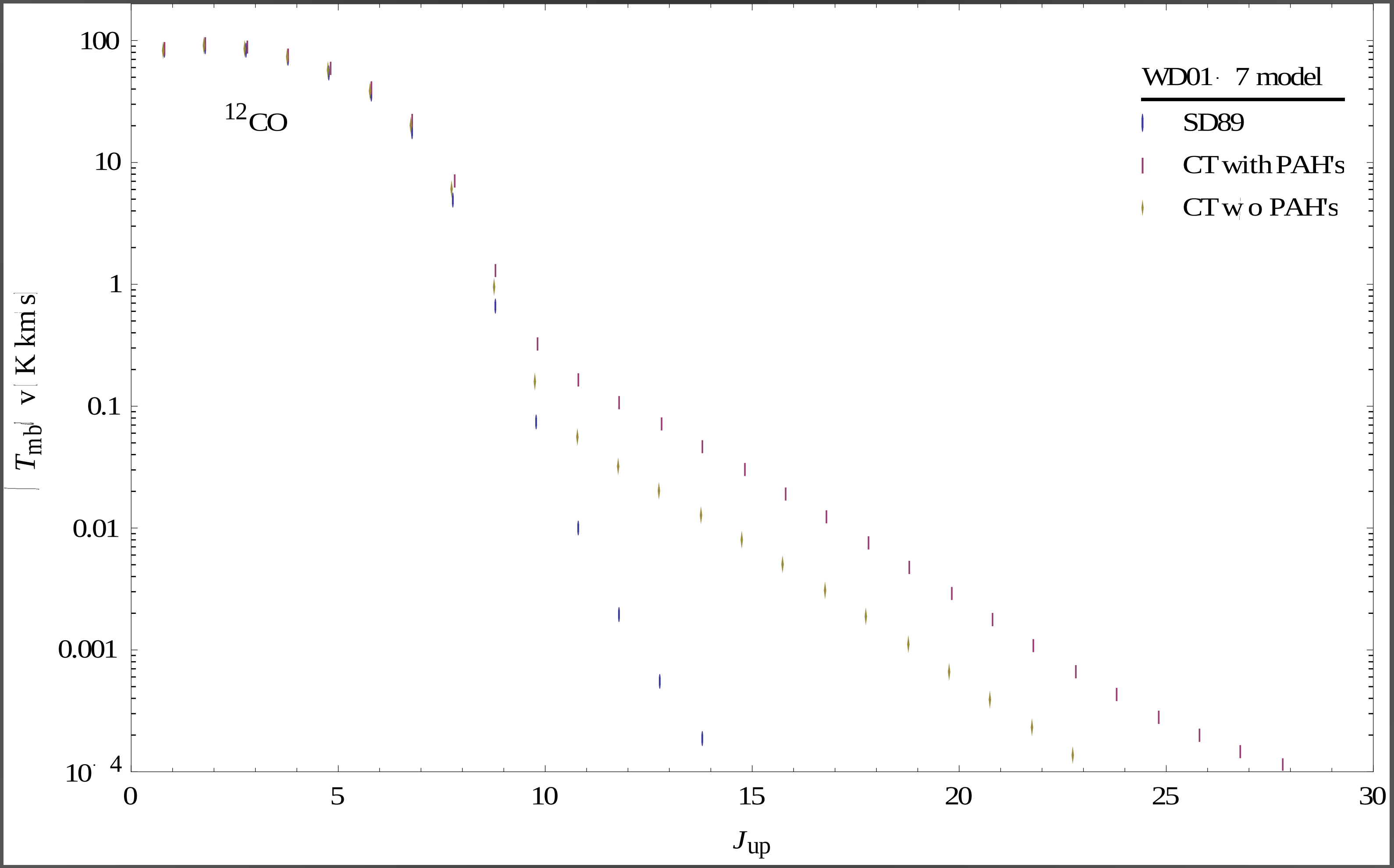

CO Surface Brightness

- New observations show that CO emission is strong even at very high-J transitions (J>20)
- Different possible excitation conditions
  - Shocks
  - PDR
  - XDR
  - Turbulence
  - plus any combination

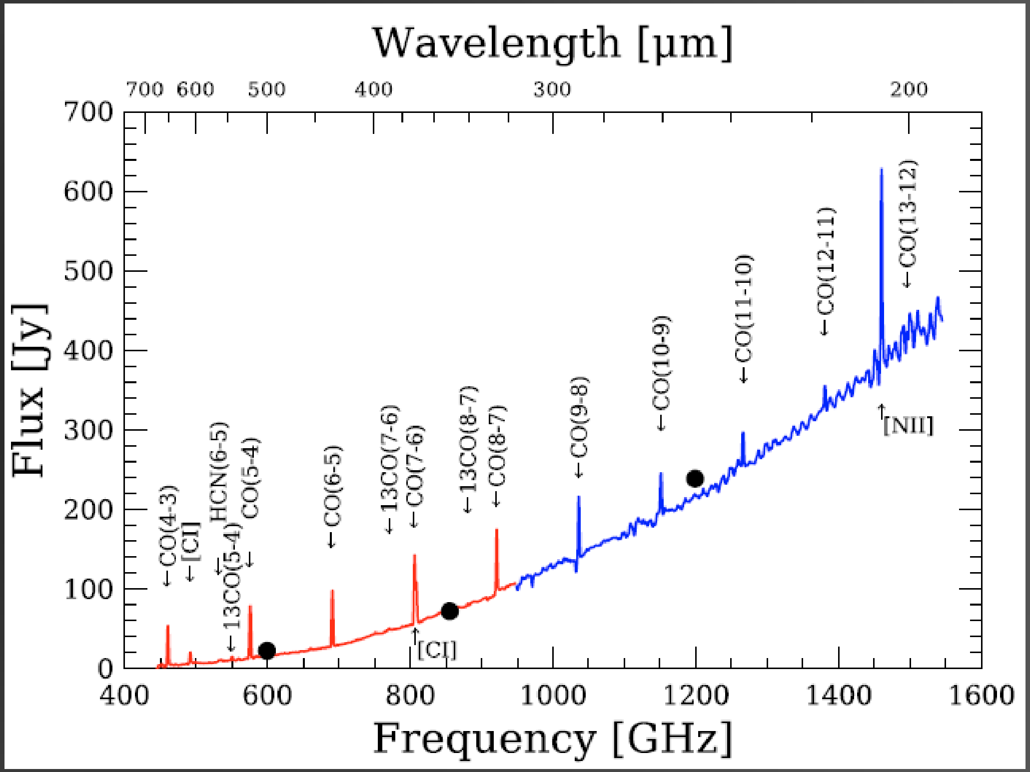

M82, Panuzzo et al. 2010 (SPIRE)

CO Surface Brightness

- New observations show strong CO emission even at very high-J transitions (J>20)

- Different possible excitation conditions
  - Shocks
  - PDR
  - XDR
  - Turbulence
  - plus any combination

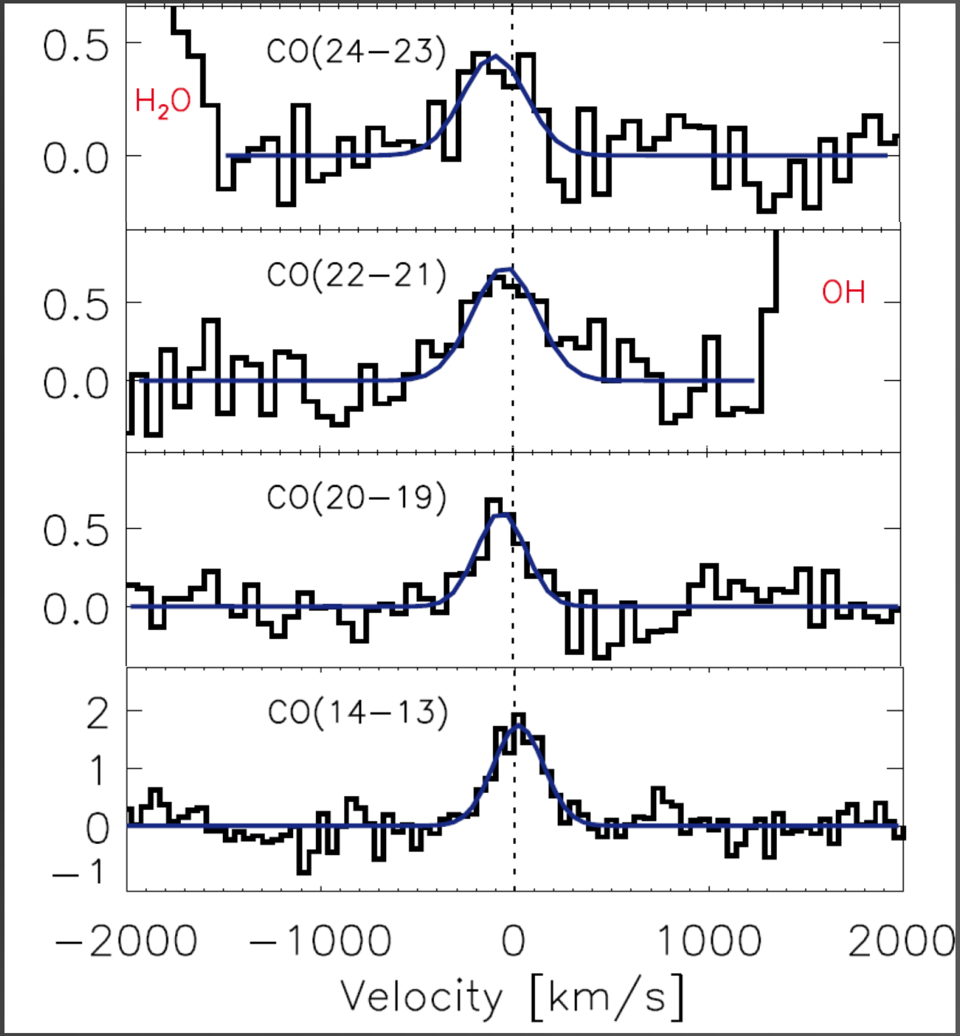

NGC 1068, Hailey-Dunsheath et al (PACS)

Model Application

Many data available

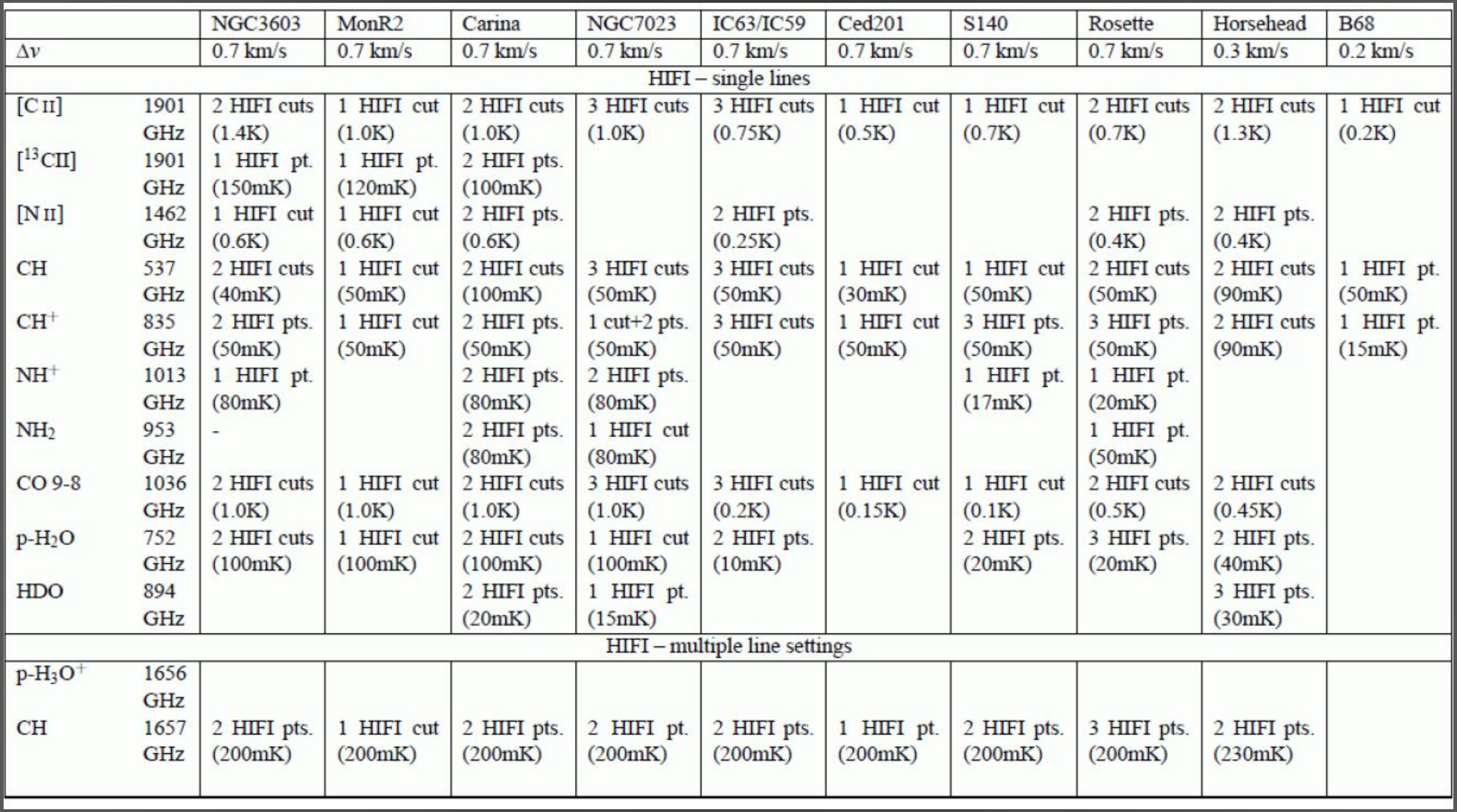

	NGC3603	MonR2	Carina	NGC7023	IC63/IC59	Ced201	S140	Rosette	Horsehead	B68
Δv	0.7 km/s	0.7 km/s	0.7 km/s	0.7 km/s	0.7 km/s	0.7 km/s	0.7 km/s	0.7 km/s	0.3 km/s	0.2 km/s
HIFI – single lines										
[C II] 1901 GHz	2 HIFI cuts (1.4K)	1 HIFI cut (1.0K)	2 HIFI cuts (1.0K)	3 HIFI cuts (1.0K)	3 HIFI cuts (0.75K)	1 HIFI cut (0.5K)	1 HIFI cut (0.7K)	2 HIFI cuts (0.7K)	2 HIFI cuts (1.3K)	1 HIFI cut (0.2K)
[^{13}CII] 1901 GHz	1 HIFI pt. (150mK)	1 HIFI pt. (120mK)	2 HIFI pts. (100mK)							
[N II] 1462 GHz	1 HIFI cut (0.6K)	1 HIFI cut (0.6K)	2 HIFI pts. (0.6K)		2 HIFI pts. (0.25K)			2 HIFI pts. (0.4K)	2 HIFI pts. (0.4K)	
CH 537 GHz	2 HIFI cuts (40mK)	1 HIFI cut (50mK)	2 HIFI cuts (100mK)	3 HIFI cuts (50mK)	3 HIFI cuts (50mK)	1 HIFI cut (30mK)	1 HIFI cut (50mK)	2 HIFI cuts (50mK)	2 HIFI cuts (90mK)	1 HIFI pt. (50mK)
CH^+ 835 GHz	2 HIFI pts. (50mK)	1 HIFI cut (50mK)	2 HIFI pts. (50mK)	1 cut+2 pts. (50mK)	3 HIFI cuts (50mK)	1 HIFI cut (50mK)	3 HIFI pts. (50mK)	3 HIFI pts. (50mK)	2 HIFI cuts (90mK)	1 HIFI pt. (15mK)
NH^+ 1013 GHz	1 HIFI pt. (80mK)		2 HIFI pts. (80mK)	2 HIFI pts. (80mK)			1 HIFI pt. (17mK)	1 HIFI pt. (20mK)		
NH_2 953 GHz	-		2 HIFI pts. (80mK)	1 HIFI cut (80mK)				1 HIFI pt. (50mK)		
CO 9-8 1036 GHz	2 HIFI cuts (1.0K)	1 HIFI cut (1.0K)	2 HIFI cuts (1.0K)	3 HIFI cuts (1.0K)	3 HIFI cuts (0.2K)	1 HIFI cut (0.15K)	1 HIFI cut (0.1K)	2 HIFI cuts (0.5K)	2 HIFI cuts (0.45K)	
p-H_2O 752 GHz	2 HIFI cuts (100mK)	1 HIFI cut (100mK)	2 HIFI cuts (100mK)	1 HIFI cut (100mK)	2 HIFI pts. (10mK)		2 HIFI pts. (20mK)	3 HIFI pts. (20mK)	2 HIFI pts. (40mK)	
HDO 894 GHz			2 HIFI pts. (20mK)	1 HIFI pt. (15mK)					3 HIFI pts. (30mK)	
HIFI – multiple line settings										
p-H_3O^+ 1656 GHz										
CH 1657 GHz	2 HIFI pts. (200mK)	1 HIFI cut (200mK)	2 HIFI pts. (200mK)	2 HIFI pt. (200mK)	2 HIFI pts. (200mK)	1 HIFI pt. (200mK)	2 HIFI pts. (200mK)	3 HIFI pts. (200mK)	2 HIFI pts. (230mK)	

Many data available

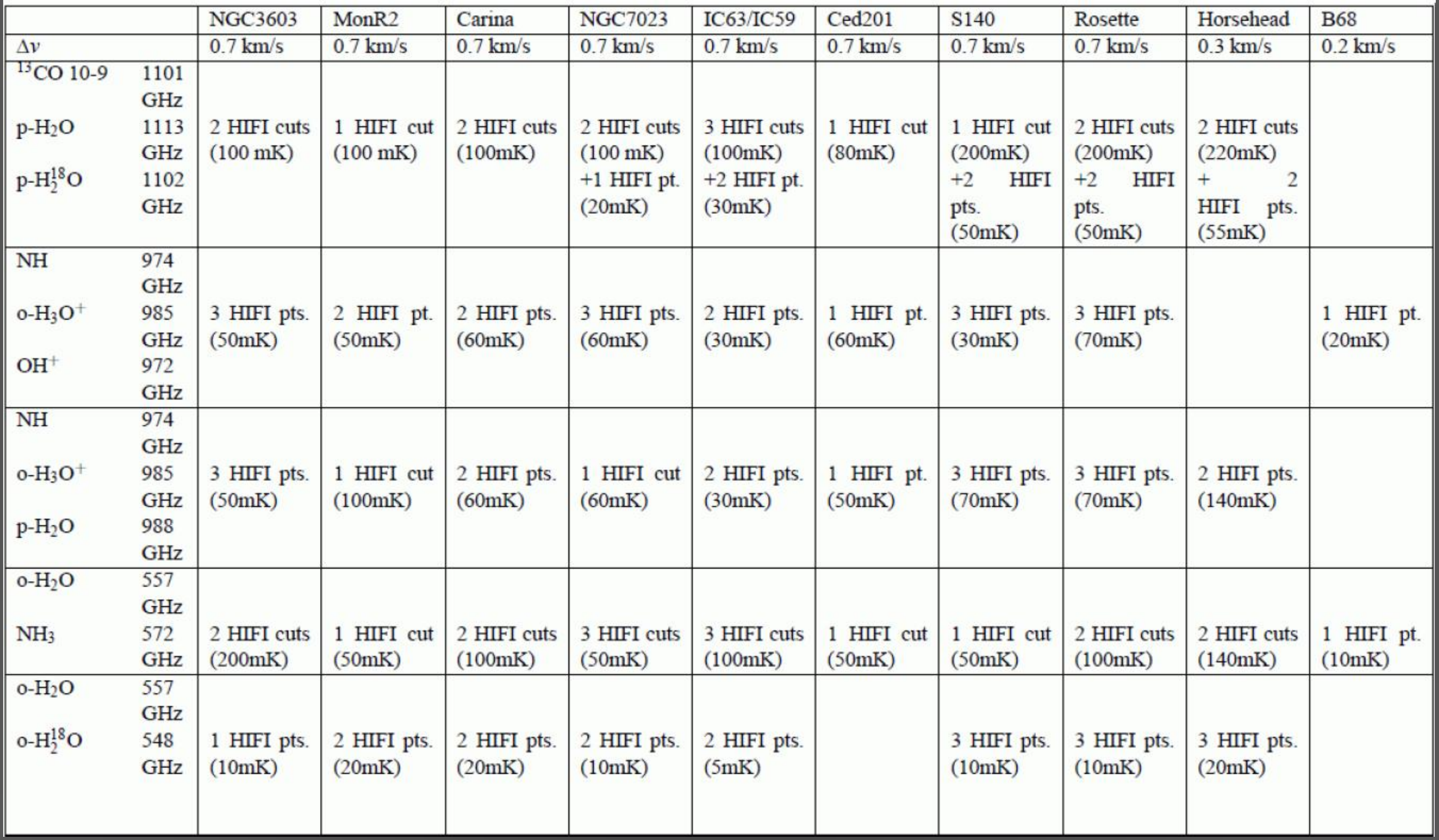

	NGC3603	MonR2	Carina	NGC7023	IC63/IC59	Ced201	S140	Rosette	Horsehead	B68
Δv	0.7 km/s	0.7 km/s	0.7 km/s	0.7 km/s	0.7 km/s	0.7 km/s	0.7 km/s	0.7 km/s	0.3 km/s	0.2 km/s
^{13}CO 10-9 1101 GHz $p\text{-}H_2O$ 1113 GHz $p\text{-}H_2^{18}O$ 1102 GHz	2 HIFI cuts (100 mK)	1 HIFI cut (100 mK)	2 HIFI cuts (100mK)	2 HIFI cuts (100 mK) +1 HIFI pt. (20mK)	3 HIFI cuts (100mK) +2 HIFI pt. (30mK)	1 HIFI cut (80mK)	1 HIFI cut (200mK) +2 HIFI pts. (50mK)	2 HIFI cuts (200mK) +2 HIFI pts. (50mK)	2 HIFI cuts (220mK) + 2 HIFI pts. (55mK)	
NH 974 GHz $o\text{-}H_3O^+$ 985 GHz OH^+ 972 GHz	3 HIFI pts. (50mK)	2 HIFI pt. (50mK)	2 HIFI pts. (60mK)	3 HIFI pts. (60mK)	2 HIFI pts. (30mK)	1 HIFI pt. (60mK)	3 HIFI pts. (30mK)	3 HIFI pts. (70mK)		1 HIFI pt. (20mK)
NH 974 GHz $o\text{-}H_3O^+$ 985 GHz $p\text{-}H_2O$ 988 GHz	3 HIFI pts. (50mK)	1 HIFI cut (100mK)	2 HIFI pts. (60mK)	1 HIFI cut (60mK)	2 HIFI pts. (30mK)	1 HIFI pt. (50mK)	3 HIFI pts. (70mK)	3 HIFI pts. (70mK)	2 HIFI pts. (140mK)	
$o\text{-}H_2O$ 557 GHz NH_3 572 GHz	2 HIFI cuts (200mK)	1 HIFI cut (50mK)	2 HIFI cuts (100mK)	3 HIFI cuts (50mK)	3 HIFI cuts (100mK)	1 HIFI cut (50mK)	1 HIFI cut (50mK)	2 HIFI cuts (100mK)	2 HIFI cuts (140mK)	1 HIFI pt. (10mK)
$o\text{-}H_2O$ 557 GHz $o\text{-}H_2^{18}O$ 548 GHz	1 HIFI pts. (10mK)	2 HIFI pts. (20mK)	2 HIFI pts. (20mK)	2 HIFI pts. (10mK)	2 HIFI pts. (5mK)		3 HIFI pts. (10mK)	3 HIFI pts. (10mK)	3 HIFI pts. (20mK)	

DR21 Geometry/Model

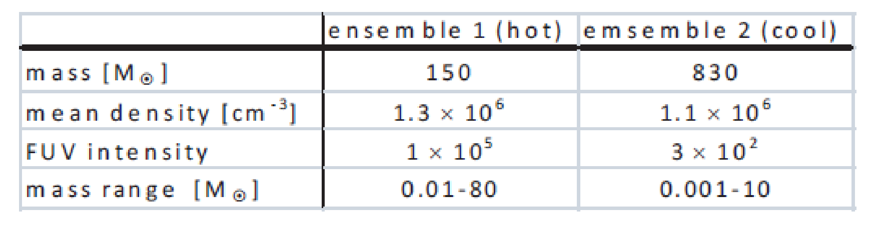

	ensemble 1 (hot)	emsemble 2 (cool)
mass [M$_\odot$]	150	830
mean density [cm^{-3}]	1.3×10^6	1.1×10^6
FUV intensity	1×10^5	3×10^2
mass range [M$_\odot$]	0.01-80	0.001-10

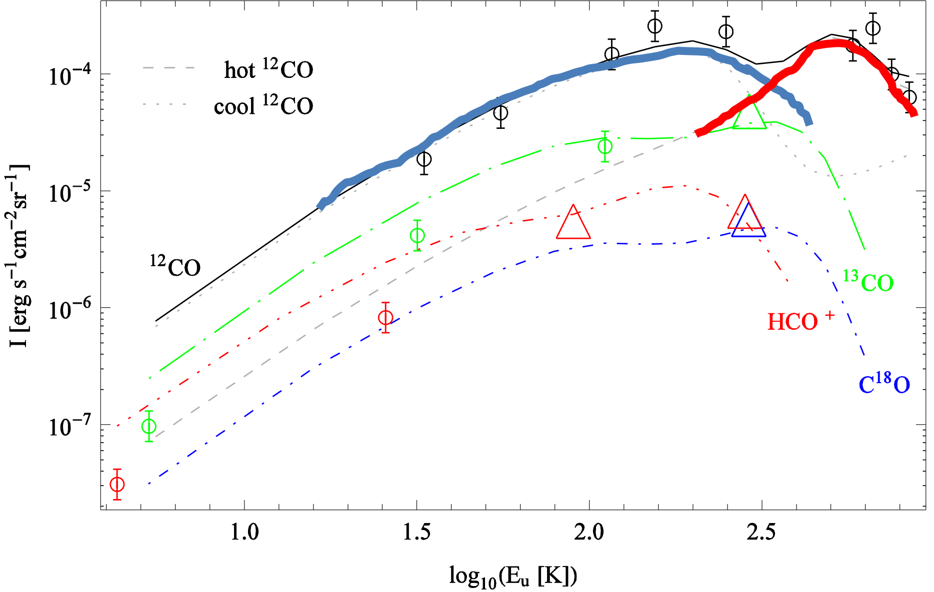

Orion Bar Geometry

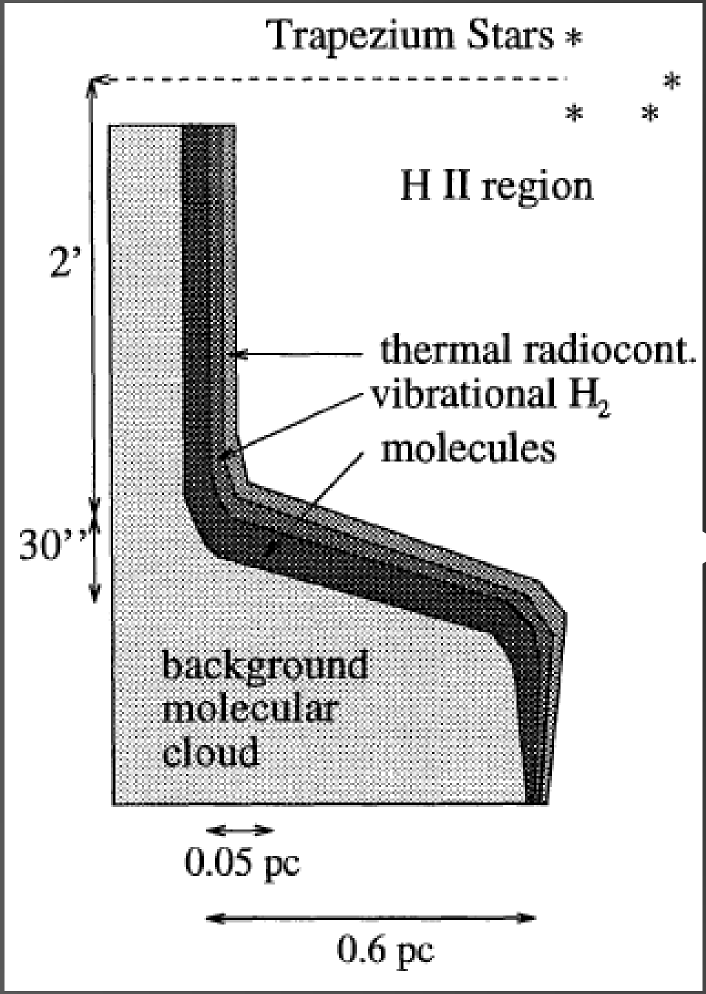

R. Visser, E. Van Dishoeck et al.

- Model: clumpy PDR *(Hogerheijde et al. 1995)*
  - $n_{\text{clump}} = 1\times10^{6}$ cm^{-3}
  - $n_{\text{interclump}} = 3\times10^{4}$ cm^{-3}
  - $G_0 = 4\times10^{4}$ *(Tielens & Hollenbach 1985)*

Orion Bar Model

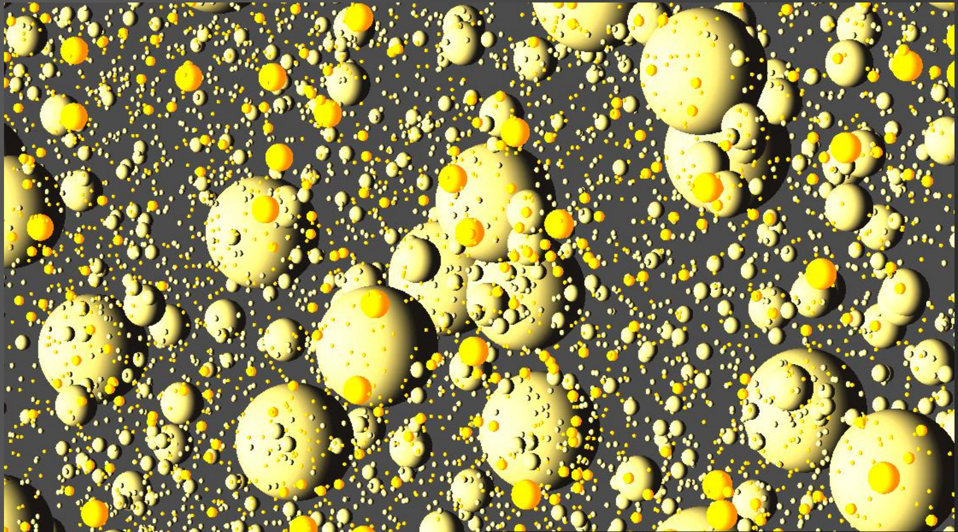

recent fit attempt (May 2011)

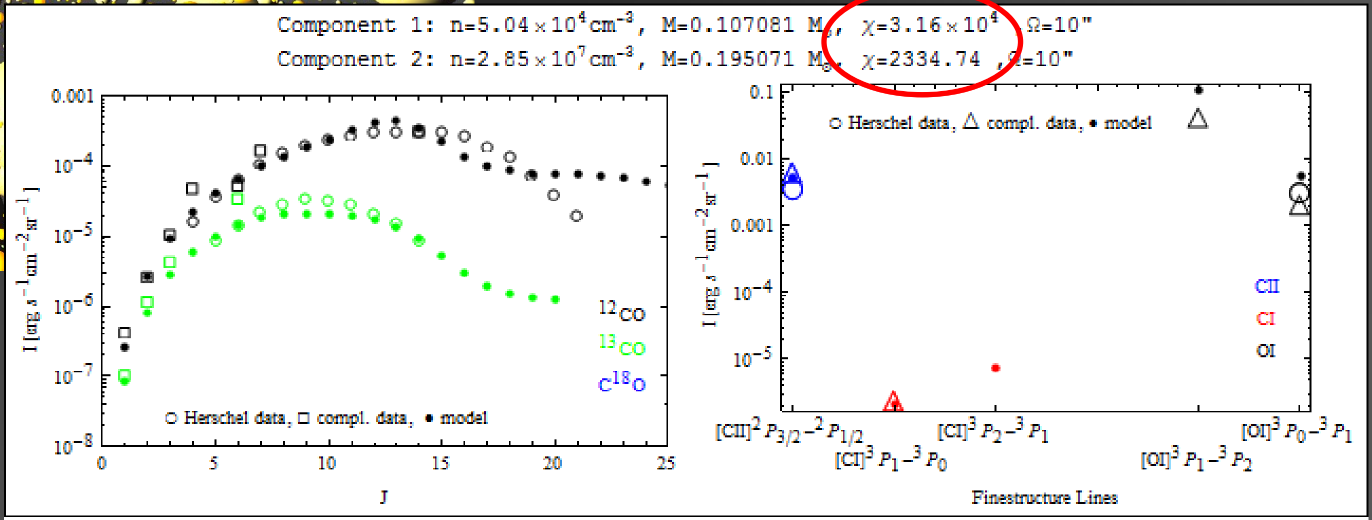

Component 1: $n=5.04\times10^{4}\,\mathrm{cm}^{-3}$, $M=0.107081\,M_\odot$, $\chi=3.16\times10^{4}$, $\Omega=10''$

Component 2: $n=2.85\times10^{7}\,\mathrm{cm}^{-3}$, $M=0.195071\,M_\odot$, $\chi=2334.74$, $\Omega=10''$

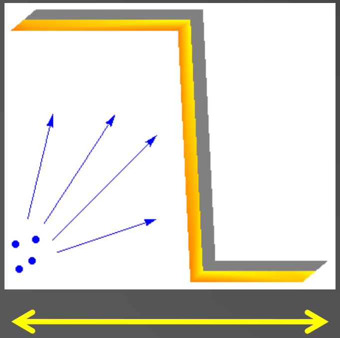

Orion Bar Model

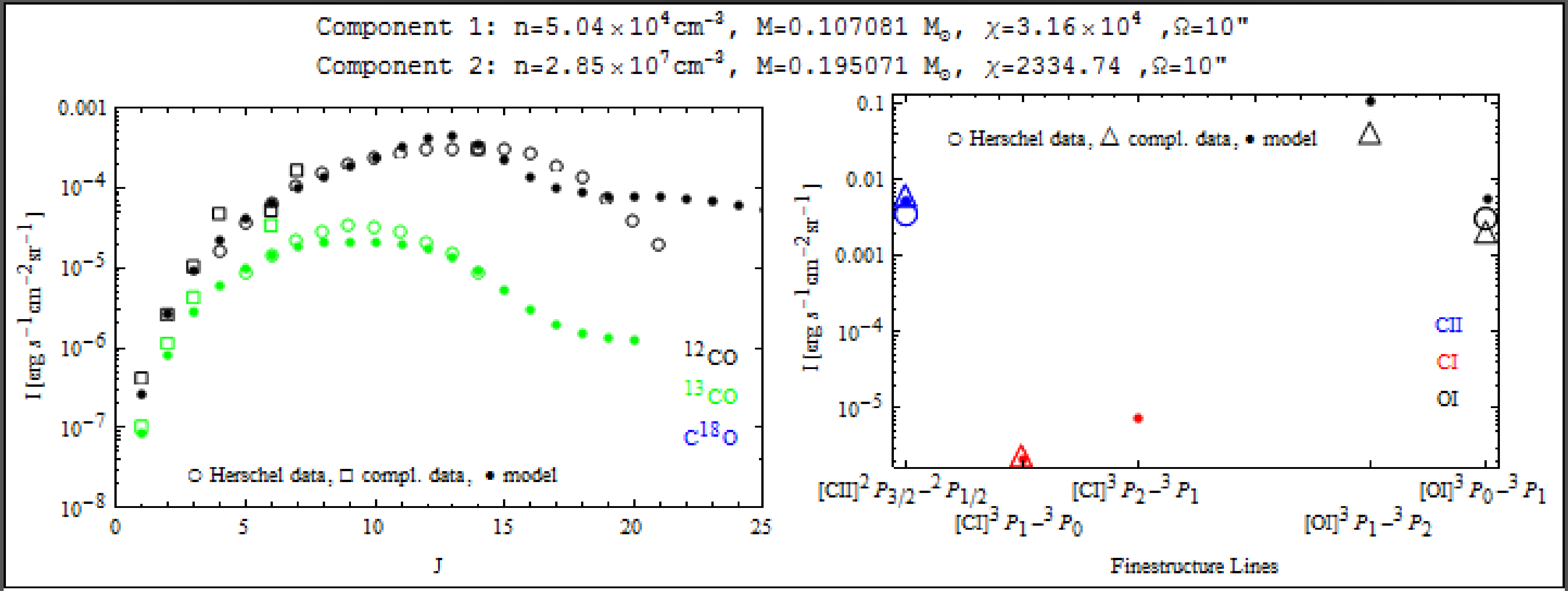

- accounting for chemisorption in H_2 formation
- dust content different from MRN
  - ⇒larger dust surface to form H_2 on
- newest CO rates

Summary

- New spectral windows teaches us a lot about the physics and chemistry in the ISM
- Growing understanding of dust properties and H_2 formation process dramatically influences model results
- Nice example of how strongly chemistry and physics are connected to each other
- “Comeback” of CO as major probe of the local conditions.

CO Excitation Workshop
PDR 4, high n, high FUV

Tgas

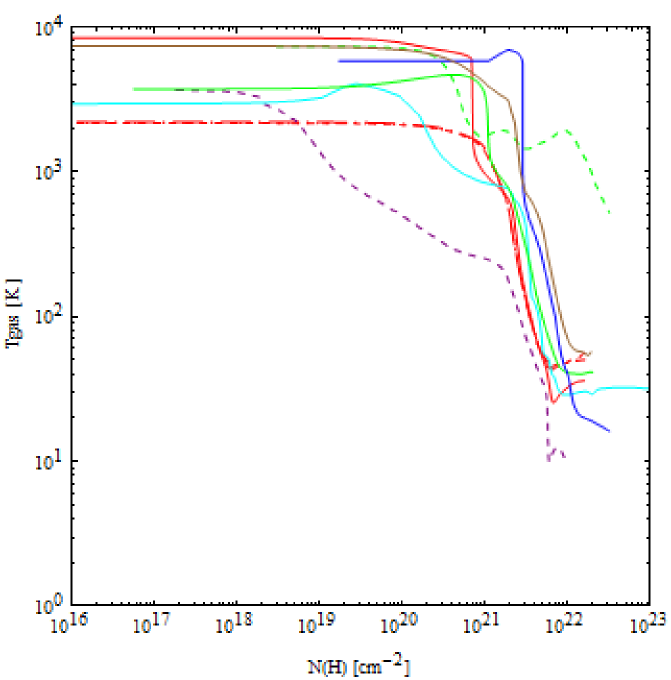

n(CO)

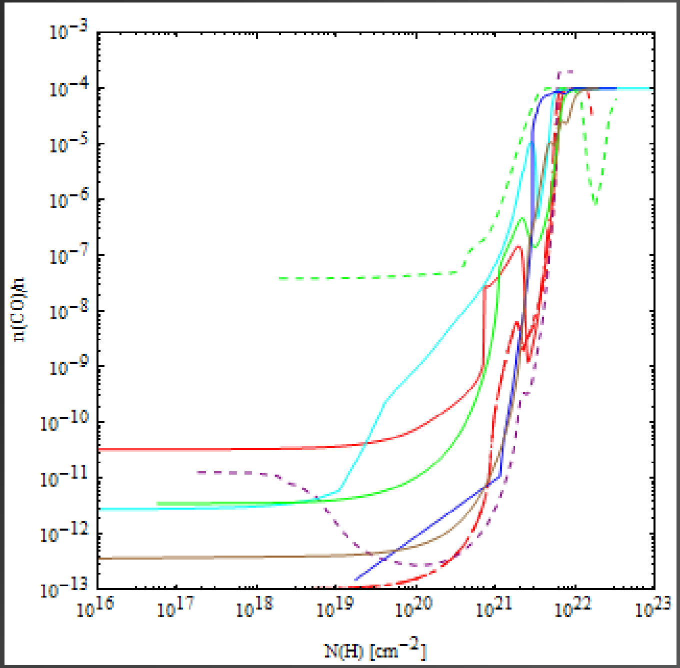

These are all benchmarked PDR codes. The scatter demonstrates the very different initial assumptions and considered physcial processe.

CO Excitation Workshop
PDR 4, high n, high FUV

NEW

Tgas

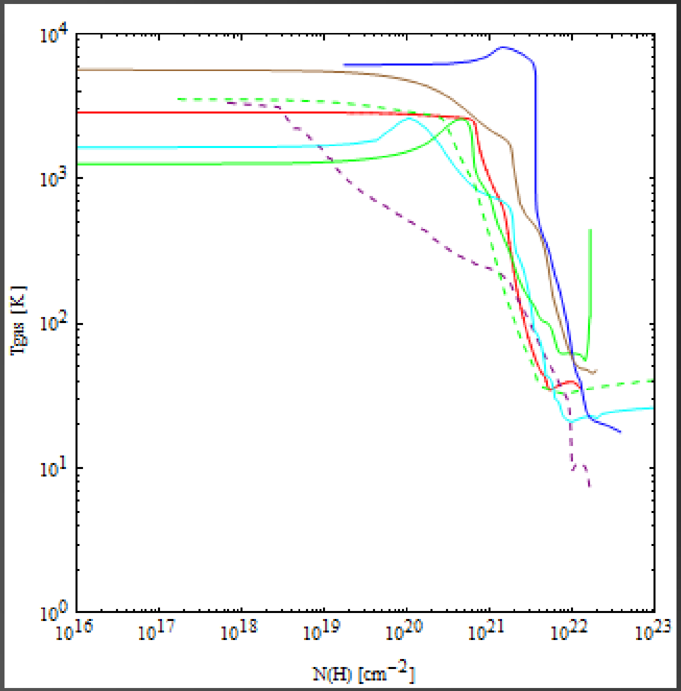

n(CO)

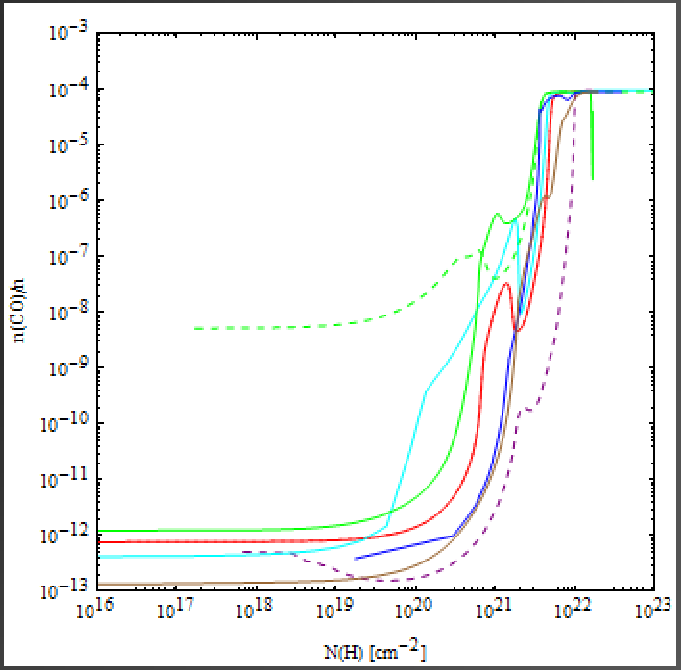

These are all benchmarked PDR codes. The scatter demonstrates the very different initial assumptions and considered physcial processes.

CO Excitation Workshop
PDR 4, high n, high FUV

NEW

PE Heating, H_2 formation heating
Dust content

Tgas

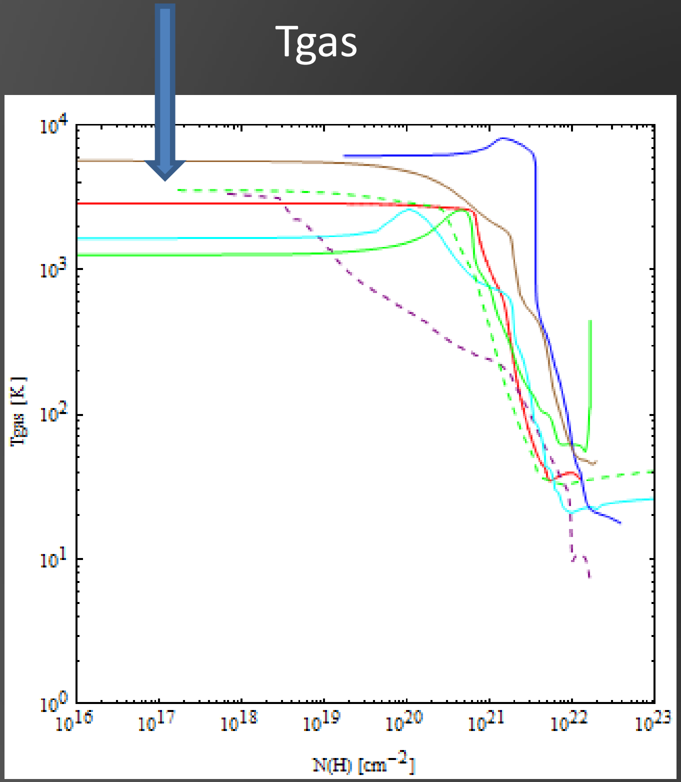

n(CO)

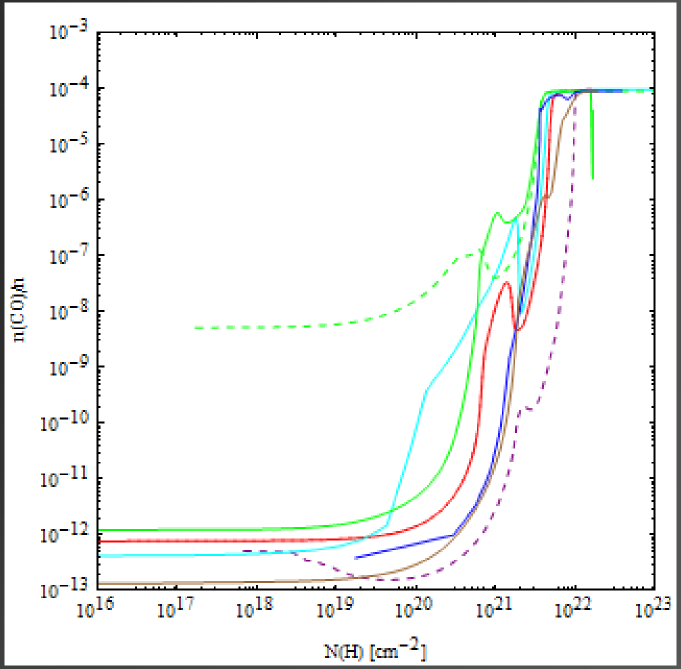

These are all benchmarked PDR codes. The scatter demonstrates the very different initial assumptions and considered physcial processes.

UMIST/UDfA - Isotopomers

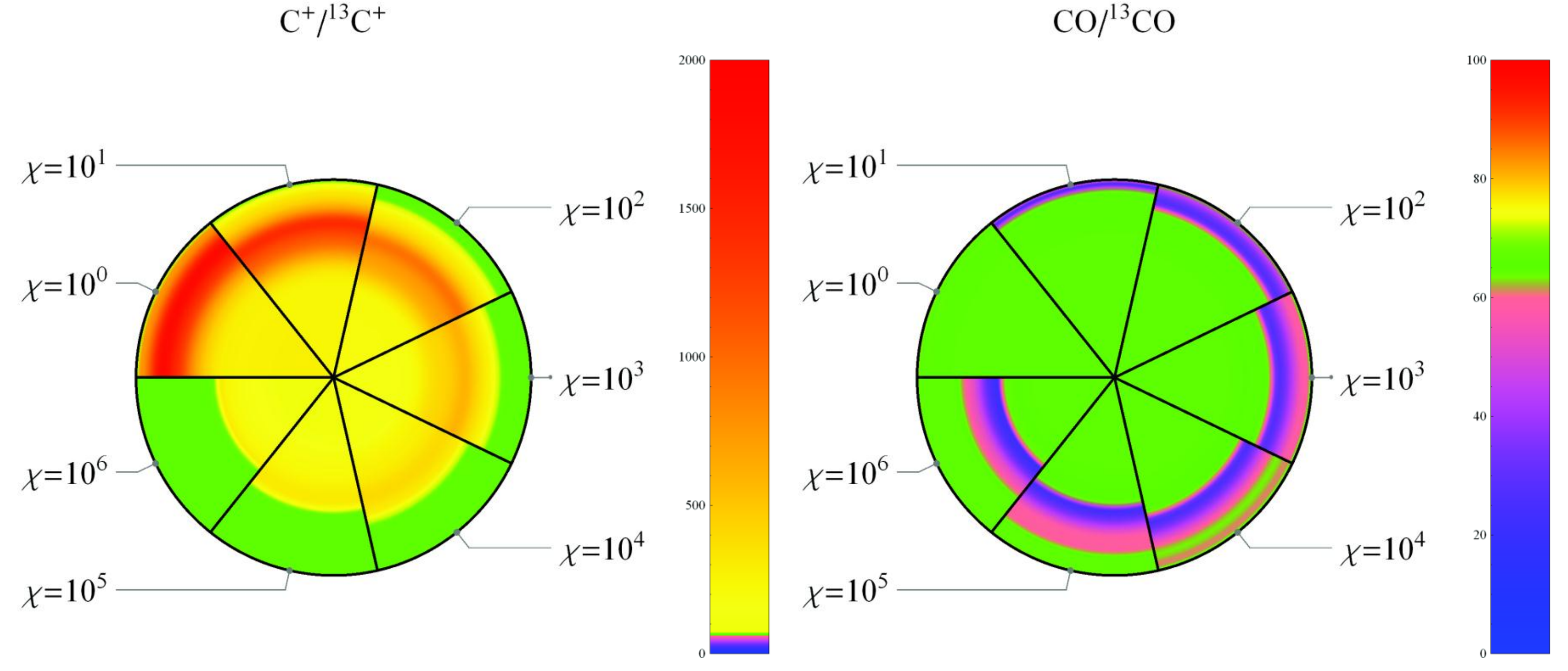

$$^{13}C^+ + {}^{12}CO \rightarrow {}^{12}C^+ + {}^{13}CO + 34.8\ K$$

Negative γ

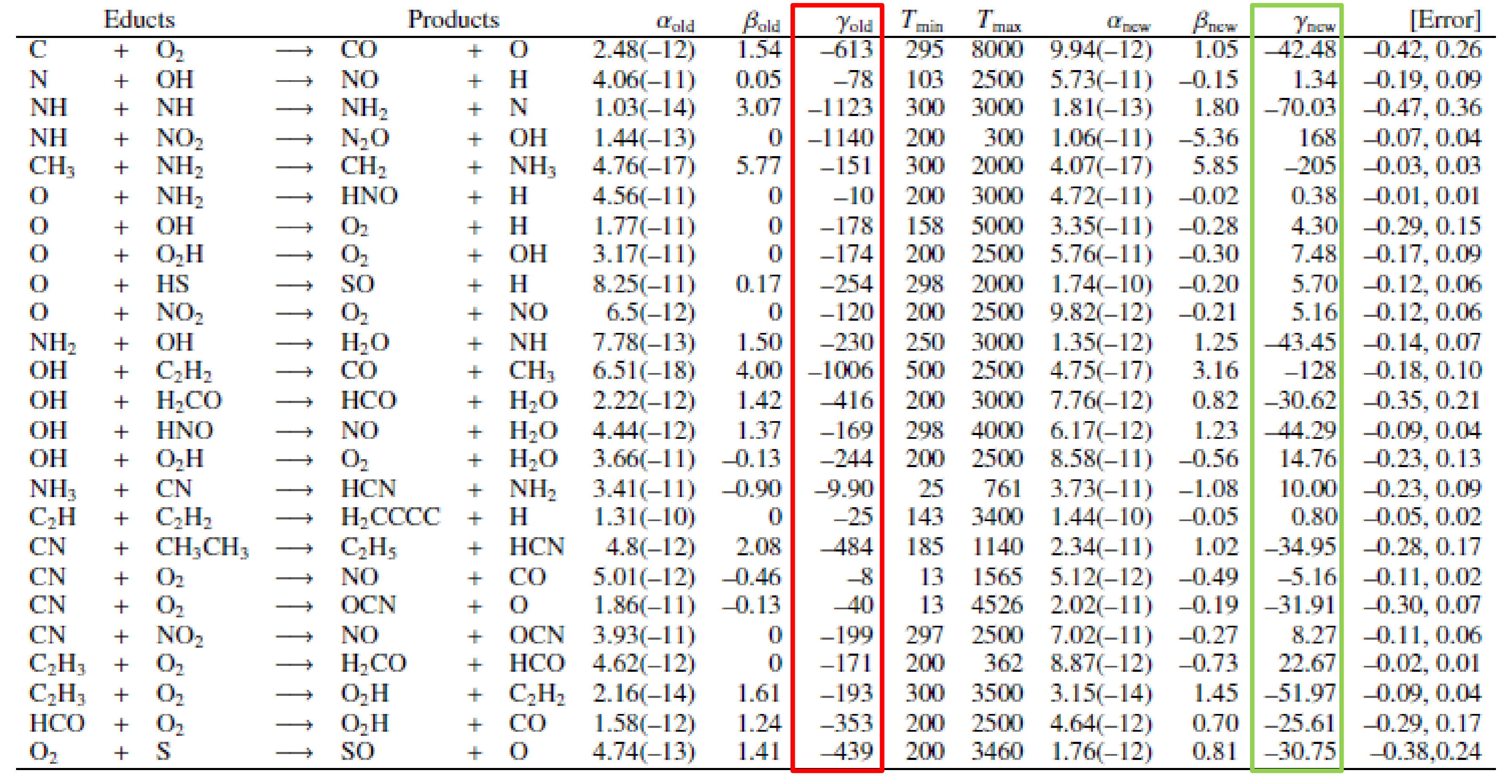

Educts				Products			$\alpha_{\rm old}$	$\beta_{\rm old}$	$\gamma_{\rm old}$	$T_{\rm min}$	$T_{\rm max}$	$\alpha_{\rm new}$	$\beta_{\rm new}$	$\gamma_{\rm new}$	[Error]
C	+	O_2	$\longrightarrow$	CO	+	O	2.48(–12)	1.54	–613	295	8000	9.94(–12)	1.05	–42.48	–0.42, 0.26
N	+	OH	$\longrightarrow$	NO	+	H	4.06(–11)	0.05	–78	103	2500	5.73(–11)	–0.15	1.34	–0.19, 0.09
NH	+	NH	$\longrightarrow$	NH_2	+	N	1.03(–14)	3.07	–1123	300	3000	1.81(–13)	1.80	–70.03	–0.47, 0.36
NH	+	NO_2	$\longrightarrow$	N_2O	+	OH	1.44(–13)	0	–1140	200	300	1.06(–11)	–5.36	168	–0.07, 0.04
CH_3	+	NH_2	$\longrightarrow$	CH_2	+	NH_3	4.76(–17)	5.77	–151	300	2000	4.07(–17)	5.85	–205	–0.03, 0.03
O	+	NH_2	$\longrightarrow$	HNO	+	H	4.56(–11)	0	–10	200	3000	4.72(–11)	–0.02	0.38	–0.01, 0.01
O	+	OH	$\longrightarrow$	O_2	+	H	1.77(–11)	0	–178	158	5000	3.35(–11)	–0.28	4.30	–0.29, 0.15
O	+	O_2H	$\longrightarrow$	O_2	+	OH	3.17(–11)	0	–174	200	2500	5.76(–11)	–0.30	7.48	–0.17, 0.09
O	+	HS	$\longrightarrow$	SO	+	H	8.25(–11)	0.17	–254	298	2000	1.74(–10)	–0.20	5.70	–0.12, 0.06
O	+	NO_2	$\longrightarrow$	O_2	+	NO	6.5(–12)	0	–120	200	2500	9.82(–12)	–0.21	5.16	–0.12, 0.06
NH_2	+	OH	$\longrightarrow$	H_2O	+	NH	7.78(–13)	1.50	–230	250	3000	1.35(–12)	1.25	–43.45	–0.14, 0.07
OH	+	C_2H_2	$\longrightarrow$	CO	+	CH_3	6.51(–18)	4.00	–1006	500	2500	4.75(–17)	3.16	–128	–0.18, 0.10
OH	+	H_2CO	$\longrightarrow$	HCO	+	H_2O	2.22(–12)	1.42	–416	200	3000	7.76(–12)	0.82	–30.62	–0.35, 0.21
OH	+	HNO	$\longrightarrow$	NO	+	H_2O	4.44(–12)	1.37	–169	298	4000	6.17(–12)	1.23	–44.29	–0.09, 0.04
OH	+	O_2H	$\longrightarrow$	O_2	+	H_2O	3.66(–11)	–0.13	–244	200	2500	8.58(–11)	–0.56	14.76	–0.23, 0.13
NH_3	+	CN	$\longrightarrow$	HCN	+	NH_2	3.41(–11)	–0.90	–9.90	25	761	3.73(–11)	–1.08	10.00	–0.23, 0.09
C_2H	+	C_2H_2	$\longrightarrow$	H_2CCCC	+	H	1.31(–10)	0	–25	143	3400	1.44(–10)	–0.05	0.80	–0.05, 0.02
CN	+	CH_3CH_3	$\longrightarrow$	C_2H_5	+	HCN	4.8(–12)	2.08	–484	185	1140	2.34(–11)	1.02	–34.95	–0.28, 0.17
CN	+	O_2	$\longrightarrow$	NO	+	CO	5.01(–12)	–0.46	–8	13	1565	5.12(–12)	–0.49	–5.16	–0.11, 0.02
CN	+	O_2	$\longrightarrow$	OCN	+	O	1.86(–11)	–0.13	–40	13	4526	2.02(–11)	–0.19	–31.91	–0.30, 0.07
CN	+	NO_2	$\longrightarrow$	NO	+	OCN	3.93(–11)	0	–199	297	2500	7.02(–11)	–0.27	8.27	–0.11, 0.06
C_2H_3	+	O_2	$\longrightarrow$	H_2CO	+	HCO	4.62(–12)	0	–171	200	362	8.87(–12)	–0.73	22.67	–0.02, 0.01
C_2H_3	+	O_2	$\longrightarrow$	O_2H	+	C_2H_2	2.16(–14)	1.61	–193	300	3500	3.15(–14)	1.45	–51.97	–0.09, 0.04
HCO	+	O_2	$\longrightarrow$	O_2H	+	CO	1.58(–12)	1.24	–353	200	2500	4.64(–12)	0.70	–25.61	–0.29, 0.17
O_2	+	S	$\longrightarrow$	SO	+	O	4.74(–13)	1.41	–439	200	3460	1.76(–12)	0.81	–30.75	–0.38,0.24

Röllig 2011, A&A 530, 9

Multiple temperature regimes

- For some reactions rate coefficients have been determined for multiple temperature regimes
- Each temp. range results in one entry in a chemical database

Multiple temperature regimes

- For some reactions rate coefficients have been determined for multiple temperature regimes
- Each temp. range results in one entry in a chemical database

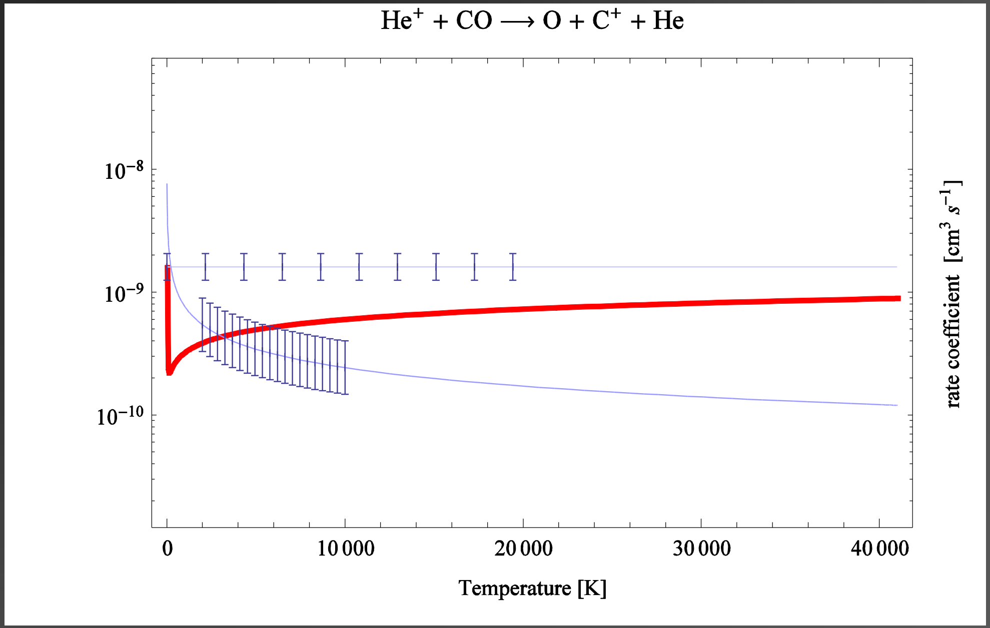

Multiple temperature regimes

- For some reactions rate coefficients have been determined for multiple temperature regimes
- Each temp. range results in one entry in a chemical database
- Moving from one temp. regime to another numerically problematic

```
C+        e-       C         PHOTON      4.67e-12   -0.60       0.0  C  10          7950        BNP97
C+        e-       C         PHOTON      1.23e-17    2.49  -21845.6  C  7950        21140       BNP97
C+        e-       C         PHOTON      9.62e-08   -1.37  115786.2C    21140       41000       BNP97
```

Multiple temperature regimes

```
C+      e-      C       PHOTON      4.67e-12   -0.60       0.0  C   10          7950        BNP97
C+      e-      C       PHOTON      1.23e-17    2.49  -21845.6  C   7950        21140       BNP97
C+      e-      C       PHOTON      9.62e-08   -1.37  115786.2C     21140       41000       BNP97
```

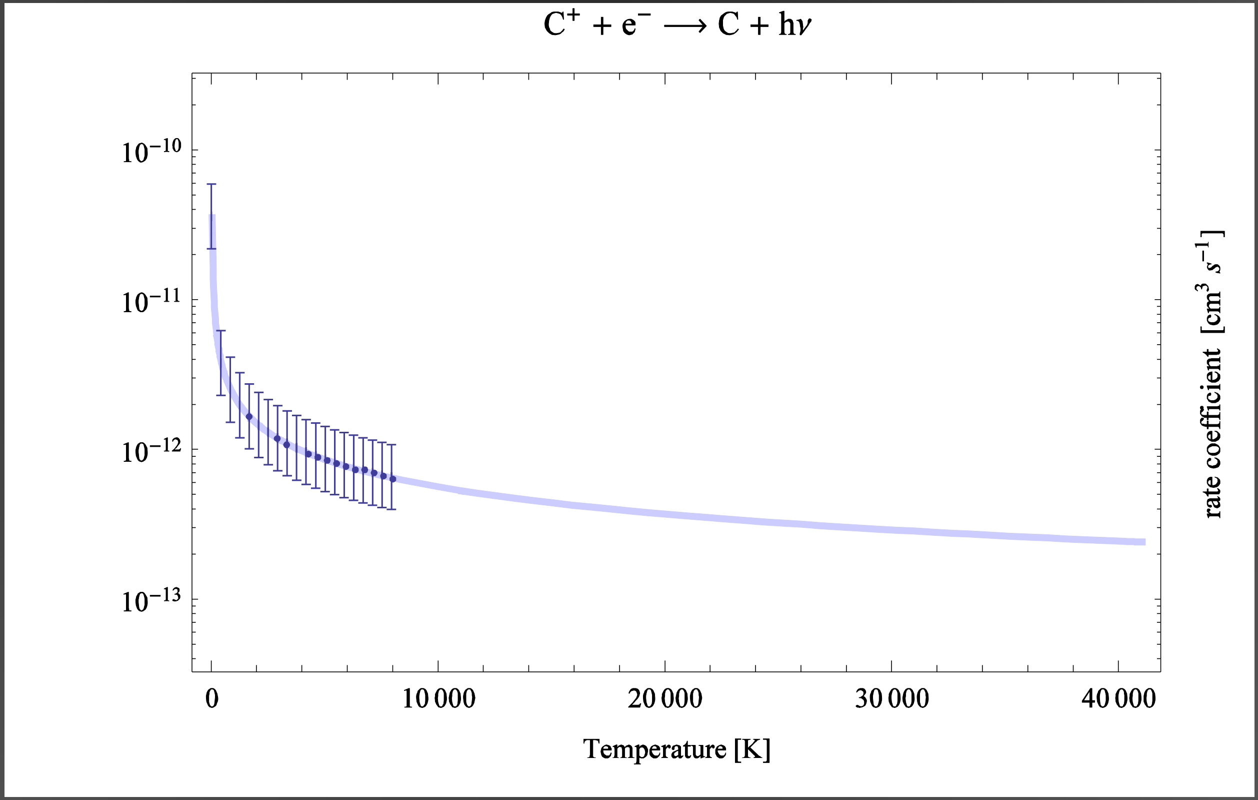

Multiple temperature regimes

```
C+      e-      C       PHOTON     4.67e-12   -0.60        0.0  C  10          7950        BNP97
C+      e-      C       PHOTON     1.23e-17    2.49   -21845.6  C  7950        21140       BNP97
C+      e-      C       PHOTON     9.62e-08   -1.37   115786.2C    21140       41000       BNP97
```

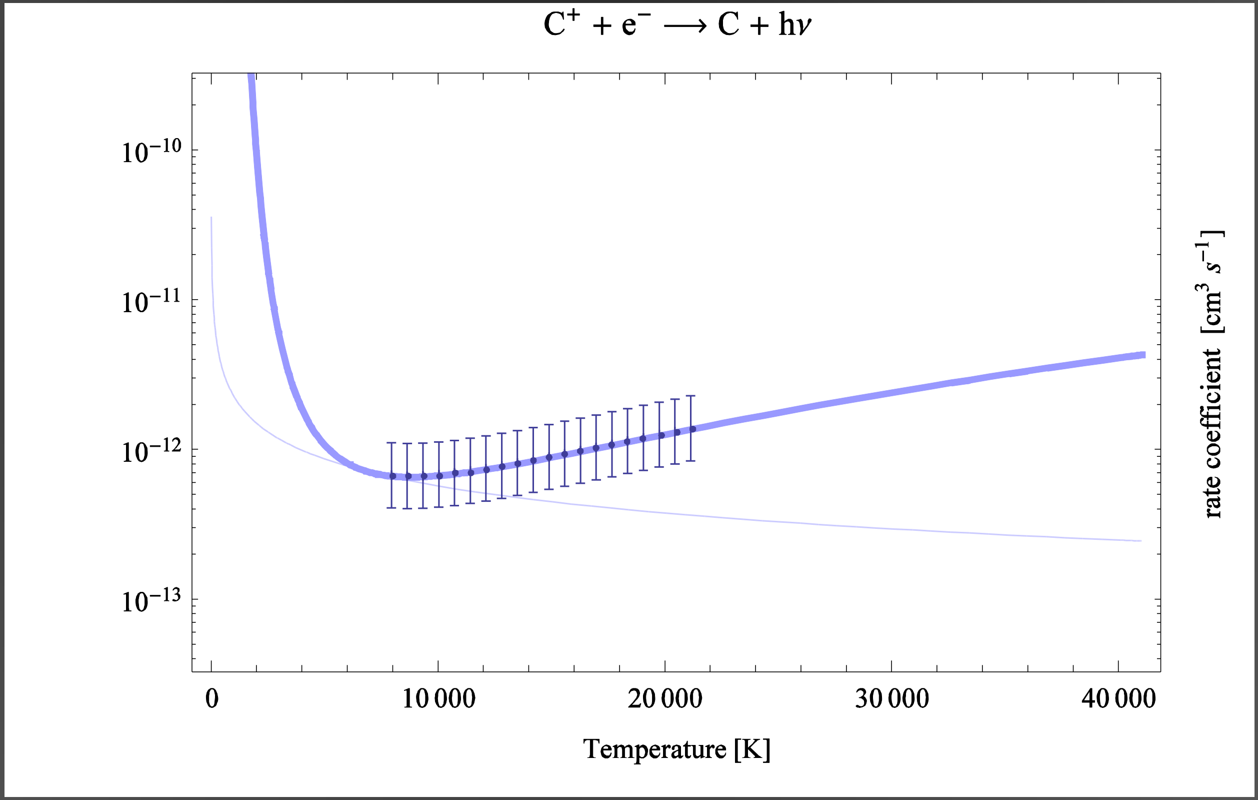

Multiple temperature regimes

```
C+      e-      C       PHOTON      4.67e-12    -0.60          0.0  C   10          7950        BNP97
C+      e-      C       PHOTON      1.23e-17     2.49    -21845.6  C   7950        21140       BNP97
C+      e-      C       PHOTON      9.62e-08    -1.37   115786.2C      21140       41000       BNP97
```

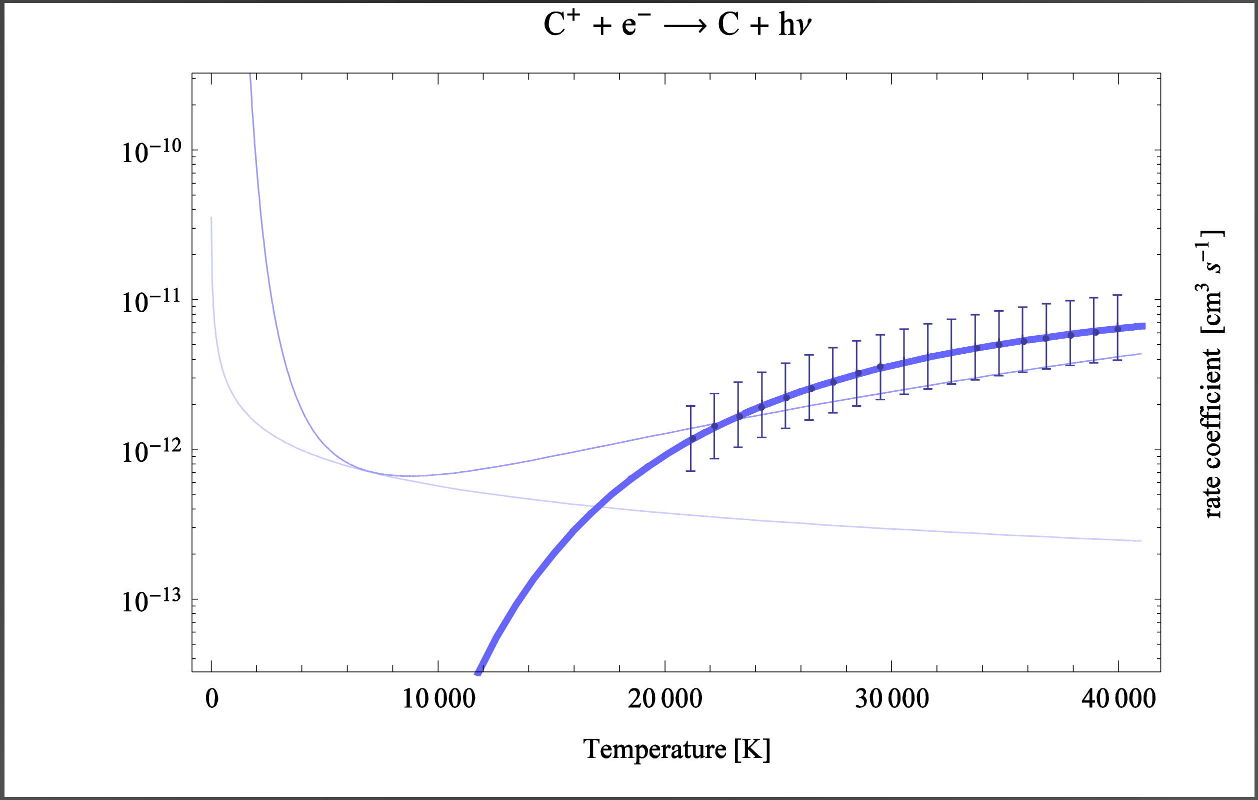

Multiple temperature regimes

```
C+      e-      C       PHOTON      4.67e-12   -0.60        0.0  C   10         7950       BNP97
C+      e-      C       PHOTON      1.23e-17    2.49   -21845.6  C   7950       21140      BNP97
C+      e-      C       PHOTON      9.62e-08   -1.37   115786.2C     21140      41000      BNP97
```

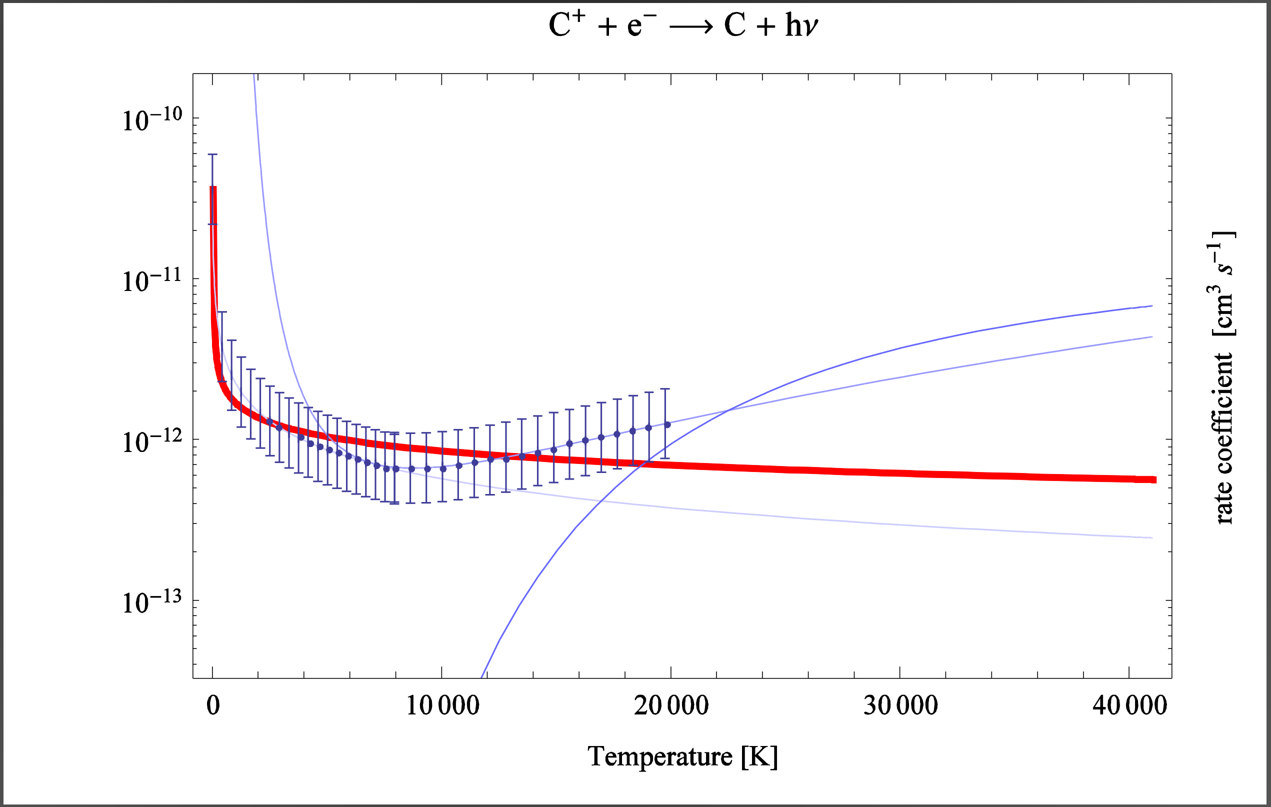

Multiple temperature regimes

```
C+        e-        C         PHOTON      4.67e-12   -0.60        0.0  C   10          7950        BNP97
C+        e-        C         PHOTON      1.23e-17    2.49   -21845.6  C   7950        21140       BNP97
C+        e-        C         PHOTON      9.62e-08   -1.37   115786.2C     21140       41000       BNP97
```

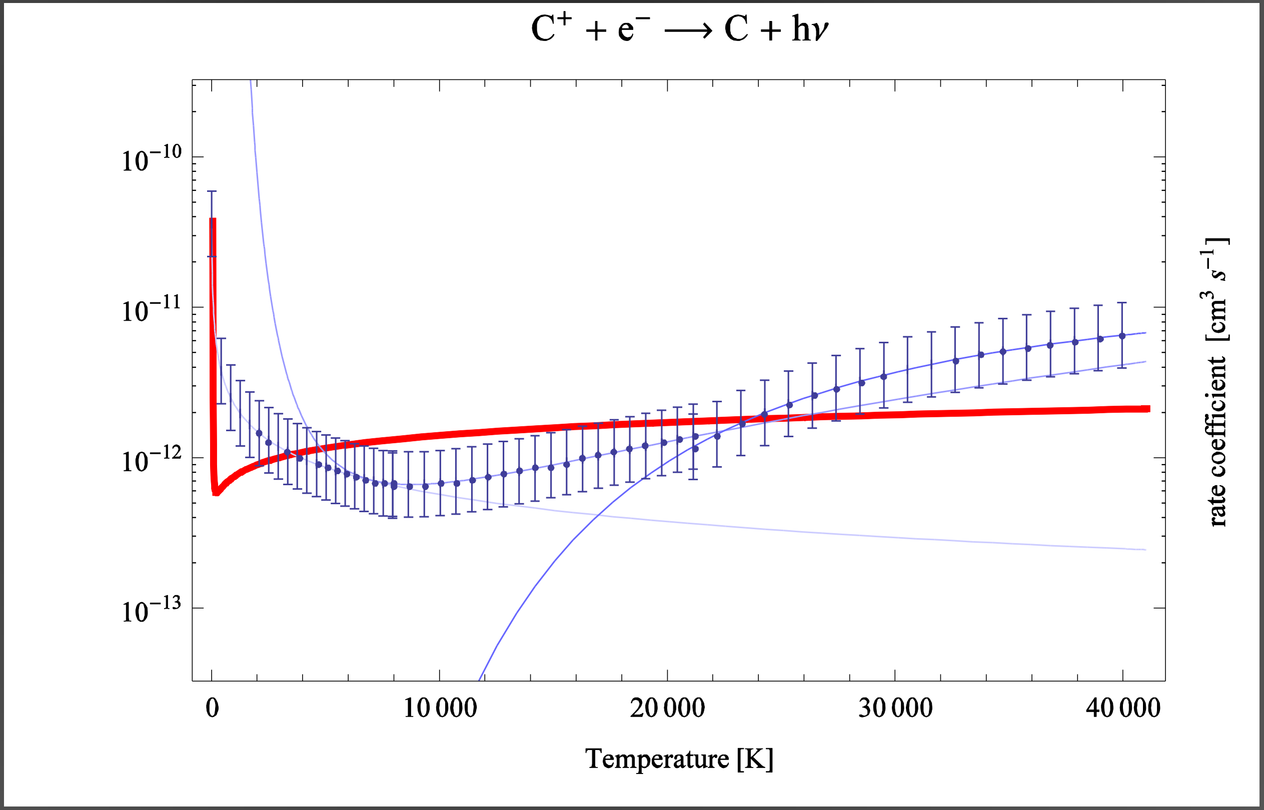

If your application requires temperatures up to 40000 K, the error grows sigificantly

Multiple temperature regimes

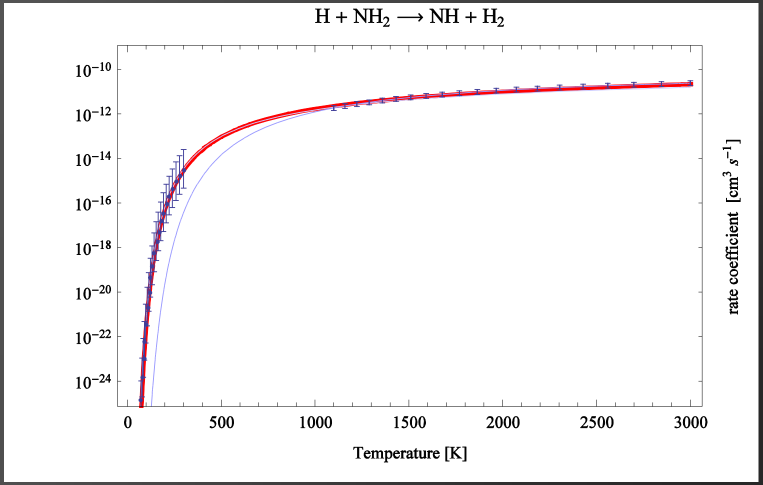
$H + NH_2 \longrightarrow NH + H_2$

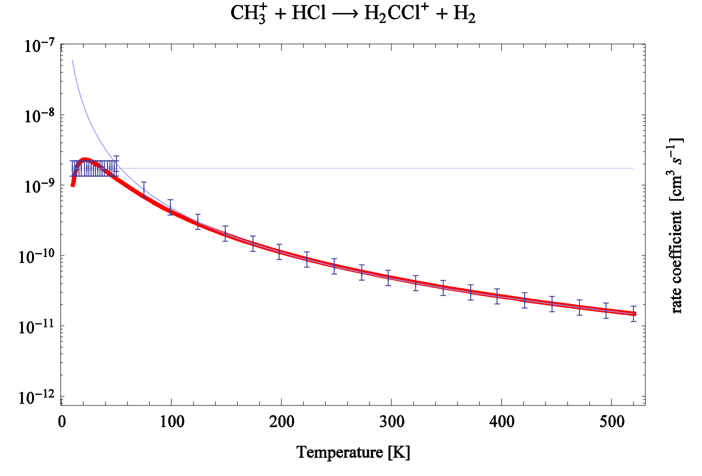
$CH_3^+ + HCl \longrightarrow H_2CCl^+ + H_2$

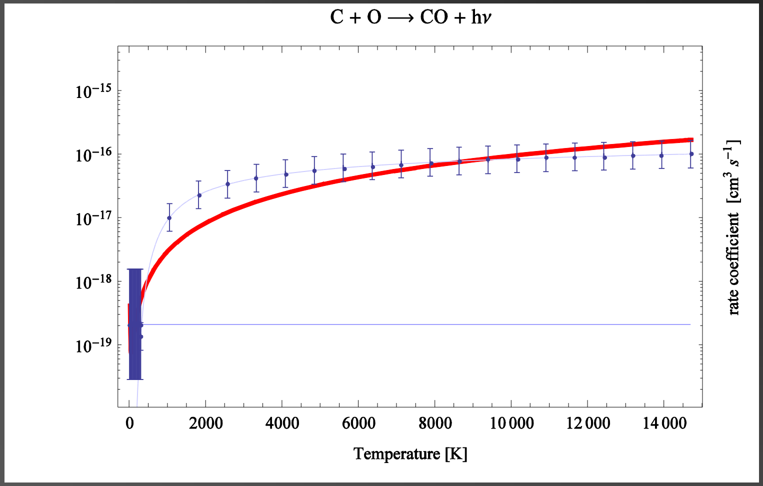
$C + O \longrightarrow CO + h\nu$

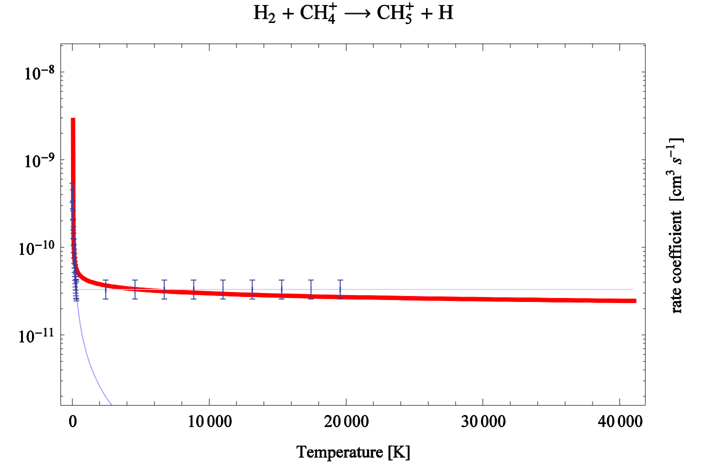
$H_2 + CH_4^+ \longrightarrow CH_5^+ + H$